

Disappointment Aversion, Term Structure, and Predictability Puzzles in Bond Markets*

Patrick Augustin[†] Roméo Tédongap[‡]

McGill University *ESSEC Business School*

May 28, 2020

Abstract

We solve a dynamic equilibrium model with generalized disappointment aversion preferences and continuous state endowment dynamics. We apply the framework to the term structure of interest rates and show that the model generates an upward sloping term structure of nominal interest rates, a downward sloping term structure of real interest rates, and that it accounts for the failure of the expectations hypothesis. The key ingredients are preferences with disappointment aversion, preference for early resolution of uncertainty, and an endowment economy with three state variables: time-varying macroeconomic uncertainty, time-varying expected inflation and inflation uncertainty.

Keywords: Asset Pricing, Macrofinance, Numerical Methods, Term Structure of Interest Rates

JEL Classification: C6, E43, E44, G12, G13

*We are grateful to the editor, Karl Diether, an anonymous associate editor, and two anonymous referees, for invaluable feedback. We also thank Dante Amengual, Giuliano Curatola, Ian Dew-Becker, Francois Gouri, Roberto Marfe, Ahn Yong Kil, and seminar participants at Syracuse University, the NEOMA Business School, the Paris December 2016 Finance Meeting, the 2nd BI-SHoF Conference in Asset Pricing and Financial Econometrics, the 33rd International Conference of the French Finance Association, the University of Gothenburg, and René Garcia's Anniversary Conference, for helpful comments and suggestions. Augustin acknowledges financial support from the Canadian Derivatives Institute. Tédongap acknowledges financial support from the French National Research Agency.

[†]McGill University - Desautels Faculty of Management, and Canadian Derivatives Institute, 1001 Sherbrooke St. West, Montreal, Quebec H3A 1G5, Canada. Email: patrick.augustin@mcgill.ca.

[‡]ESSEC Business School Paris-Singapore, 3 Avenue Bernard Hirsch, 95021 Cergy-Pontoise, France. Email: tedongap@essec.edu.

1 Introduction

Asymmetric preferences over losses and gains make investors take decisions that are inconsistent with the predictions of expected utility theory (i.e., the Allais paradox). Such behavior can be rationalized by introducing aversion to disappointing outcomes into axiomatic models of decision making under uncertainty (Gul; 1991). Models that incorporate such asymmetries into preferences have successfully rationalized various asset pricing anomalies.

Routledge and Zin (2010), for example, show how the endogenous variation in disappointment probability, induced by preferences with disappointment aversion, produces sufficiently large countercyclical risk aversion to jointly explain the equity and risk-free rate puzzles of Mehra and Prescott (1985) and Weil (1989). Bonomo et al. (2011) show that persistent fluctuations in macroeconomic uncertainty together with asymmetric preferences generate realistic stock return moments and predictability patterns without time-varying expected growth. Augustin and Tédongap (2016) illustrate how asymmetric preferences improve the fit of the conditional moments of sovereign credit spreads, while Campanale et al. (2010) study the implications of disappointment aversion preferences for equity prices and the short rate in a production economy. Other successful applications relate to cross-sectional equity pricing anomalies (Delikouras; 2017) and portfolio choice problems (Dahlquist et al.; 2017).¹

A discontinuity in preferences, implied by the disappointment threshold and characterized through a kink in the indifference curve, complicates the analytical derivation of asset pricing formulas. One common solution in prior work is, therefore, a discrete state approximation of the economy.² While discrete regime-switching models approximate continuous processes well in population (Timmermann; 2000), they are less useful for studying the small sample properties of highly persistent processes. However, to match asset prices, recursive

¹Furthermore, Farago and Tédongap (2018) decompose expected excess returns into their regular and downside risk components, while Delikouras (2014) and Schreindorfer (2019) use disappointment preferences to price defaultable bonds and options. Dolmas (2013) combines disappointment aversion with rare disasters.

²In a special case with central disappointment aversion and homoscedastic consumption growth, Delikouras (2017) provides a closed-form solution to the welfare valuation ratios using the Campbell and Shiller (1988b) log-linear approximation of the return to the claim on aggregate consumption.

utility frameworks often rely on highly persistent processes, especially for the dynamics of consumption growth volatility. Moreover, the incorporation of asymmetric preferences with disappointment aversion into asset pricing models with persistent shocks to economic fundamentals is growing because of their success in resolving multiple asset pricing puzzles jointly. This growing number of applications calls for a solution method when the state of the economy is continuous, consistent with observed dynamics. We propose such a method, because standard log-linearizations may result in quantitatively important pricing errors, especially in the presence of persistent shocks (Pohl et al.; 2018). Moreover, it is not obvious that standard approximation methods such as projection onto Chebyshev polynomials or perturbation methods handle the discontinuity in the preferences well (Aruoba et al.; 2006).

We first solve a general framework that allows for a solution to asset prices when preferences feature non-linearities and the endowment dynamics are continuous in state-dependent outcomes. We then apply the framework to the term structures of real and nominal interest rates because the upward sloping term structure of interest rates depends significantly on the propagation of persistent shocks to risk premia at multiple horizons. In such circumstances, solving models without log-linear approximations may be preferable (Pohl et al.; 2018).

In our benchmark framework, we propose a parsimonious model of real aggregate consumption growth with only one single state variable, the volatility of aggregate consumption growth. Consumption growth is non-predictable and features an affine GARCH model for macroeconomic uncertainty. Thus, we assume that realized consumption growth and economic uncertainty are impacted by the same shock. This feature allows us to limit the resolution of asset prices to a one-dimensional numerical integration. In an extension, we explore the asset pricing implications when consumption growth is predictable and its conditional mean is modulated by the same shock that drives real growth and uncertainty.

We also specify an exogenous inflation process for the pricing of nominal assets. Realized inflation has a time-varying mean, and the innovations in both realized and expected inflation are perfectly positively correlated, implying an ARMA(1,1) process for realized

inflation. Like macroeconomic uncertainty, inflation uncertainty follows affine GARCH dynamics. While inflation innovations do not affect future consumption growth, innovations in consumption growth are contemporaneously correlated with realized and expected inflation. In the benchmark model, nominal prices rely on only three state variables: time-varying macroeconomic uncertainty, time-varying expected inflation and inflation uncertainty.

The model matches the observed evidence of an upward (downward) sloping term structure of nominal interest rates (volatilities), computed using Fama-Bliss zero-coupon bond prices between 1964 and 2018. We obtain an upward sloping nominal yield curve if inflation is negatively correlated with innovations in aggregate consumption growth and if the agent prefers early resolution of uncertainty. If consumption is negatively correlated with expected inflation, agents will borrow from future consumption by issuing bonds. This drives down nominal bond prices and increases nominal yields. In our model, the impact of expected inflation is attenuated at longer horizons and, thus, long-term bonds are less sensitive to expected inflation shocks than short-term bonds. On the other hand, bond yields respond negatively to a rise in inflation uncertainty, and more so for longer-maturity bonds. This suggests a flight-to-quality effect in response to nominal uncertainty. Similarly, an increase in real uncertainty increases nominal bond prices and lowers nominal yields. The magnitude of the impact depends on the asset horizon and is greater for shorter maturities. Thus, the flight-to quality effect dominates the intertemporal substitution effect because higher consumption volatility lowers nominal yields. The slope of the term structure of real interest rates is negative, consistent with the intuition that inflation-indexed bonds provide a hedge against future consumption. Thus, agents are willing to pay a premium to hold such assets, which implies a negative risk premium.

Our model also accounts for the failure of the expectations hypothesis. We replicate different versions of the regressions that have confirmed the existence of predictability in bond returns using simulated data with 300,000 monthly observations. We quantitatively match the regression coefficients and explanatory power implied by the projection of holding

period returns on the single Cochrane and Piazzesi (2005) factor, the Fama and Bliss (1987) regressions of holding period returns on forward-spot spreads, the Campbell and Shiller (1991) regressions of changes in long rate spreads on yield-spot spreads, and by the Dai and Singleton (2002) regressions of adjusted changes in long rate spreads on yield-spot spreads.

The success of our model relies partly on its ability to generate both time-varying prices and quantities of risk. This is a desirable feature for equilibrium models, as pointed out by Le and Singleton (2013) and Creal and Wu (2020). The model endogenously generates time-varying prices of risk because the disappointment threshold is a function of the certainty equivalent of future lifetime utility. As the certainty equivalent evolves dynamically, the pricing kernel implied by the disappointment aversion preferences exhibits endogenously time-varying market prices of risk. We also show theoretically that the kink in the indifference curve, which arises from the asymmetry in preferences, introduces a volatility of the pricing kernel that is at least as large as that of an investor with symmetrically recursive preferences as in Epstein and Zin (1989). These features generate strongly time-varying and countercyclical risk aversion that help quantitatively match the predictability patterns in nominal bond returns.

Our work relates most closely to Piazzesi and Schneider (2006) and Bansal and Shaliastovich (2013), who study the term structure of nominal interest rates in endowment economies with symmetric recursive utility. In contrast to their work, we examine the impact of asymmetric recursive utility preferences that account for endogenously time-varying disappointment. In addition, in our benchmark model, consumption growth is non-predictable, but embeds time-varying real uncertainty. Piazzesi and Schneider (2006) specify consumption growth dynamics that are homoscedastic and predictable. Bansal and Shaliastovich (2013) allow for time-variation in the mean and volatility of expected growth, while the conditional volatility of consumption growth is constant. In extensions of our model, we show that we match the moments of the term structure of interest rates using similar specifications. However, it is challenging to reconcile the failure of the expectations hypothesis without time-

varying consumption growth volatility, while a model with predictable consumption growth generates too much predictability of future consumption growth by the price-dividend ratio (Beeler and Campbell; 2012).

In Section 2, we discuss the solution method for a representative agent equilibrium model with generalized disappointment aversion preferences and a continuous state endowment economy. We apply the framework to the term structure of real and nominal interest rates in Section 3. In Section 4, we discuss the results and illustrate implications for the predictability of bond returns. We provide model extensions in Section 5 and compare our results to those from existing models of the term structure of interest rates. We conclude in Section 6.

2 Model

We describe the generalized disappointment aversion (GDA) preferences of Routledge and Zin (2010) in Section 2.1 and characterize a general framework for the endowment dynamics in Section 2.2. We discuss the numerical solution method in Section 2.3.

2.1 Preferences and Stochastic Discount Factor

The representative agent exhibits aversion for disappointing outcomes. Such preferences are based on the work of Gul (1991) and are generalized by Routledge and Zin (2010). As in Epstein and Zin (1989) and Weil (1989), the investor derives utility V_t recursively from the level of current aggregate consumption C_t and the certainty equivalent of next period lifetime utility $\mathcal{R}_t(V_{t+1})$, which captures the utility over all future consumption streams:

$$\begin{aligned} V_t &= \left\{ (1 - \delta) C_t^{1 - \frac{1}{\psi}} + \delta [\mathcal{R}_t(V_{t+1})]^{1 - \frac{1}{\psi}} \right\}^{\frac{1}{1 - \frac{1}{\psi}}} \quad \text{if } \psi \neq 1 \\ &= C_t^{1 - \delta} [\mathcal{R}_t(V_{t+1})]^\delta \quad \text{if } \psi = 1, \end{aligned} \tag{2}$$

where $0 < \delta < 1$ captures the time preference and $\psi > 0$ characterizes the elasticity of intertemporal substitution.

The agent has asymmetric preferences over good and bad outcomes because she dislikes disappointing events, notably by assigning a penalty weight to these outcomes when forming her certainty equivalent. More specifically, with GDA preferences, the risk-adjustment function $\mathcal{R}(V)$ is implicitly defined by:

$$U(\mathcal{R}) = E[U(\mathcal{R})] - \ell E[(U(\kappa\mathcal{R}) - U(V))I(V < \kappa\mathcal{R})], \quad (3)$$

where $I(\cdot)$ is an indicator function defined to be one if the condition is met and zero otherwise, and where the utility function $U(\cdot)$ is defined as:

$$U(C) = (1 - \gamma)^{-1} C^{1-\gamma} \quad \text{if } \gamma > 0 \quad \text{and } \gamma \neq 1, \quad (4)$$

where $\gamma > 0$ is the coefficient of relative risk aversion. When $\gamma = 1$, $U(C) = \ln(C)$. The coefficient of generalized disappointment aversion, $0 < \kappa \leq 1$, defines the fraction of the certainty equivalent below which an outcome is considered to be disappointing, while the coefficient of disappointment aversion $\ell \geq 0$ defines by how much utility is reduced in disappointing states. With ℓ equal to zero, the model nests the symmetric Kreps and Porteus (1978) expected utility certainty equivalent \mathcal{R} , and V_t is restored to be the standard Epstein and Zin (1989) recursive utility. When $\ell > 0$, outcomes below a fraction κ of the certainty equivalent \mathcal{R} lower the utility by an amount modulated by ℓ .

From Equation (3), it follows that the risk-adjusted future lifetime utility may be rewritten as:

$$\mathcal{R}_t(V_{t+1}) = \left(E_t \left[\frac{1 + \ell I(V_{t+1} < \kappa \mathcal{R}_t(V_{t+1}))}{1 + \ell \kappa^{1-\gamma} E_t[I(V_{t+1} < \kappa \mathcal{R}_t(V_{t+1}))]} V_{t+1}^{1-\gamma} \right] \right)^{\frac{1}{1-\gamma}}, \quad (5)$$

where $E_t[\cdot]$ denotes the expectation conditional on all information available at time t . Hansen et al. (2007) derive the stochastic discount factor $M_{t,t+1}$ in terms of the continuation value

of utility of consumption as:

$$M_{t,t+1} = M_{t,t+1}^* \left(\frac{1 + \ell I(V_{t+1} < \kappa \mathcal{R}_t(V_{t+1}))}{1 + \ell \kappa^{1-\gamma} E_t[I(V_{t+1} < \kappa \mathcal{R}_t(V_{t+1}))]} \right), \quad (6)$$

where

$$M_{t,t+1}^* = \delta \left(\frac{C_{t+1}}{C_t} \right)^{-\frac{1}{\psi}} \left(\frac{V_{t+1}}{\mathcal{R}_t(V_{t+1})} \right)^{\frac{1}{\psi} - \gamma}. \quad (7)$$

2.2 Generalized Endowment Economy

Let $\mathcal{O}(\cdot; \cdot)$ and $\mathcal{S}(\cdot; \cdot)$ be two generic functions describing the observation and the state equations. The dynamics of real aggregate consumption growth $\Delta c_{t+1} = \ln(C_{t+1}/C_t)$ are described by the following state-space system:

$$\begin{aligned} \Delta c_{t+1} &= \mathcal{O}(\mathcal{E}_{t+1}; \mathbf{X}_t) \\ \mathbf{X}_{t+1} &= \mathcal{S}(\mathcal{E}_{t+1}; \mathbf{X}_t), \end{aligned} \quad (8)$$

with \mathbf{X}_t defining an N -dimensional real-valued vector process governing the state of the real economy, and \mathcal{E}_{t+1} defining a K -dimensional vector of independent and identically distributed shocks with density function $h(\mathcal{E})$ and support $\mathbb{E} \subseteq \mathbb{R}^K$.

2.3 Model Solution

We need to find a solution to the welfare valuation ratios V_t/C_t and $\mathcal{R}_t(V_{t+1})/C_t$, which define the lifetime utility and the certainty equivalent of future lifetime utility to the current consumption level, respectively. These ratios are functions of the N -dimensional state vector \mathbf{X}_t that governs the real economy. In this section, we explain how to explicitly solve for the welfare valuation ratios, which allow for the derivation of the probability of disappointment and the stochastic discount factor. We relegate technical expressions to Appendix A.

Given a specification of the endowment process as defined in Equation (8), we solve for

the welfare valuation ratios:

$$V_t/C_t = G^V(\mathbf{X}_t) \quad \text{and} \quad \mathcal{R}_t(V_{t+1})/C_t = G^{\mathcal{R}}(\mathbf{X}_t), \quad (9)$$

conjecturing that they are functions of the N -dimensional state vector \mathbf{X}_t . From the recursion in Equation (2), it follows that $G^V = F(G^{\mathcal{R}})$, where

$$\begin{aligned} F(G) &= \left\{ (1 - \delta) + \delta G^{1 - \frac{1}{\psi}} \right\}^{\frac{1}{1 - \frac{1}{\psi}}} \quad \text{if } \psi \neq 1, \\ &= G^\delta \quad \text{if } \psi = 1 \end{aligned} \quad (10)$$

for any positive real number G . Hence the first step is to derive a solution to $G^{\mathcal{R}}$, the ratio of the certainty equivalent of future lifetime utility to the current consumption level. We explicitly show in Appendix A that $G^{\mathcal{R}}(\mathbf{X}_t)$ is the solution to a fixed-point equation that can be solved recursively using numerical integration, based on a grid of values for the vector process \mathbf{X}_t . Our method is conceptually similar to the one used by Campbell and Cochrane (1999) to solve for the price-consumption ratio in the external habit model, and is referred to as the *fixed-point* method by Wachter (2005).³

Specifically, we initiate the recursion by conjecturing a solution to $G_0^{\mathcal{R}}(\mathbf{X}_t)$. Given $k \geq 1$, $G_k^{\mathcal{R}}(\mathbf{X}_t)$ is then obtained on a grid of values for \mathbf{X}_t , following which we iterate forward. At each step of the recursion, we evaluate the function obtained in the previous iteration at a set of points $\mathcal{S}(\mathcal{E}_{t+1}; \mathbf{X}_t)$ for each value of \mathbf{X}_t , where $\{\mathcal{E}_{t+1}\}$ is determined by the numerical integration routine. Typically, these points lie outside the predefined grid of values for \mathbf{X}_t . Thus, we apply an interpolation method to evaluate $G_{k-1}^{\mathcal{R}}$ at these points.⁴ The solution to the recursion yields a fixed point for $G^{\mathcal{R}}(\mathbf{X}_t)$, which is unique (Backus et al.; 2004; Marinacci

³Wachter (2005) compares the advantages of the *fixed point* and *series* methods for the speed of convergence of the solution to the price-consumption ratio. That comparison is impossible in our framework as the welfare valuation ratios follow a non-linear recursion that cannot be expressed as a sum of recursive terms.

⁴One example is the log-linear interpolation method, assuming that $\ln G^{\mathcal{R}}(\mathbf{X}_t)$ is linear in \mathbf{X}_t . This interpolation method is similar to the one used in Campbell and Cochrane (1999) to numerically solve the habit formation model.

and Montrucchio; 2010).

Based on the solution of $G^{\mathcal{R}}$, we derive the solution of $G^V = F(G^{\mathcal{R}})$. It is then straightforward to compute the disappointment probability $\xi_t \equiv \xi(\mathbf{X}_t)$ and the real stochastic discount factor $M_{t,t+1} \equiv M(\mathbf{X}_t, \mathbf{X}_{t+1}, \Delta c_{t+1})$, which are derived using the solutions to the welfare valuation ratios V_t/C_t and $\mathcal{R}_t(V_{t+1})/C_t$. Detailed expressions are reported in Equations (A.7) and (A.8) of Appendix A, respectively.

3 Application to the Term Structure of Interest Rates

We solve for the real and nominal yield curves in Section 3.1, and specify an explicit model for consumption growth and inflation in Section 3.2. Calibrations and data are described in Section 3.3.

3.1 Asset Prices: Real and Nominal Yield Curves

The price of an n -period real zero-coupon bond must satisfy the Euler equation

$$P_{n,t} = E_t[M_{t,t+n}]. \quad (11)$$

We solve for the term structure of real interest rates recursively, given our conjecture that $P_{n,t} = P_n(\mathbf{X}_t)$, and that the n -period real zero-coupon bond satisfies the recursion

$$P_n(\mathbf{X}_t) = E_t[M_{t,t+1}P_{n-1}(\mathbf{X}_{t+1})], \quad (12)$$

with the initial condition $P_{0,t}(\mathbf{X}_t) = 1$. Real bond prices are computed recursively using numerical integration, and we report detailed expressions in Equation (B.2) of Appendix B. Given the solution for real bond prices, real yields of maturity n are defined as $y_{n,t} = -(n)^{-1} p_{n,t}$, where $p_{n,t}$ is the natural logarithm of the real bond price.

Nominal assets are priced by discounting future nominal payoffs with the nominal stochastic discount factor, the logarithm of which is the difference between the logarithm of the real pricing kernel, $m_{t,t+1} \equiv \ln M_{t,t+1}$, and the inflation rate π_{t+1} , i.e., $m_{t,t+1}^\$ = m_{t,t+1} - \pi_{t+1}$. Similar to the price of the real zero-coupon bond, the price of an n -period nominal zero-coupon bond $P_{n,t}^\$$ satisfies the recursion

$$P_{n,t}^\$ = E_t [M_{t,t+1}^\$ P_{n-1,t+1}^\$], \quad (13)$$

with initial condition given by $P_{0,t}^\$ = 1$.

For the analysis of nominal prices, we specify a process for inflation π_{t+1} that embeds a rich class of affine inflation dynamics as specified in Wachter (2006), Piazzesi and Schneider (2006), Koijen et al. (2010), and Bansal and Shaliastovich (2013), among others. To derive the solution to nominal bond prices, we assume that the inflation dynamics are governed by an L -dimensional real-valued vector process \mathbf{Y}_t such that the joint moment generating function, conditional on the real vector of shocks \mathcal{E}_{t+1} , is given by:

$$E_t [\exp (a\pi_{t+1} + b^\top \mathbf{Y}_{t+1}) \mid \mathcal{E}_{t+1}] = \exp (A(a, b, \mathbf{X}_t, \mathcal{E}_{t+1}) + \mathbf{Y}_t^\top H^\$(a, b)), \quad (14)$$

which we use to conjecture that:

$$P_{n,t}^\$ = P_n^\$(\mathbf{X}_t) \exp (\mathbf{Y}_t^\top B_n^\$), \quad (15)$$

where the coefficients $B_n^\$$ satisfy the recursion $B_n^\$ = H^\$(-1, B_{n-1}^\$)$, with the initial vector-valued condition $B_0^\$ = \mathbf{0}$. We use the law of iterated expectations to ensure that the numerical integration applies only to the vector of real shocks \mathcal{E}_t , which allows us to show that $P_n^\$(\mathbf{X}_t)$ satisfies the recursion

$$P_n^\$(\mathbf{X}_t) = E_t [M_{t,t+1}^\$ P_{n-1}^\$(\mathbf{X}_{t+1}) \exp (A(-1, B_{n-1}^\$, \mathbf{X}_t, \mathcal{E}_{t+1}))], \quad (16)$$

with initial condition $P_0^\$ (\mathbf{X}_t) = 1$. Detailed expressions for nominal bond prices are reported in Equation (B.6) of Appendix B. Given the solution for nominal bond prices, nominal yields to maturity n are defined as $y_{n,t}^\$ = -(n)^{-1} p_{n,t}^\$$, where $p_{n,t}^\$ \equiv \ln P_{n,t}^\$$ is the natural logarithm of the nominal bond price.

3.2 An Explicit Model for Consumption Growth and Inflation

For the application of our framework, we specify an explicit process for the endowment and inflation, characterized by Equations (8) and (14), respectively. Solving models of generalized disappointment aversion with continuous state endowment dynamics requires numerical solution methods. This implies that solutions to asset prices involve integration over the support of each independent source of risk. This computational complexity makes a parsimonious model attractive and desirable. We thus present a model where the state of the real economy is characterized by a single state variable σ_t , the volatility of aggregate consumption growth. The existence of fluctuations in macroeconomic uncertainty is now well established (Kandel and Stambaugh; 1990; Stock and Watson; 2002) and its importance for asset prices and the real economy has been demonstrated, among many others, by Bansal et al. (2005), Lettau et al. (2008), Bloom (2009), and Jurado et al. (2015). We show that such a parsimonious framework together with asymmetry in preferences is powerful enough to explain the salient features of the term structure of interest rates and return predictability in bond markets. Our results in the bond market echo those found for the stock market. Specifically, Bonomo et al. (2011) illustrate that, in the absence of persistent fluctuations in the mean of aggregate consumption growth, a recursive utility model with a generalized disappointment aversion certainty equivalent improves empirical return predictability patterns in the stock market over a specification with an expected utility certainty equivalent and long run risk in expected consumption growth.

We model real aggregate growth Δc_{t+1} to have a constant mean μ_c and affine GARCH

variance dynamics, following Heston and Nandi (2000).⁵ Assuming GARCH instead of, for example, stochastic volatility dynamics, avoids multi-dimensional integration when we numerically solve for asset prices. In addition, it guarantees the desirable feature of a positive volatility process under specific parameter restrictions. Formally, the real economy is characterized by:

$$\begin{aligned}\Delta c_{t+1} &= \mathcal{O}(\varepsilon_{t+1}; \sigma_t^2) = \mu_c + \sigma_t \varepsilon_{t+1} \\ \sigma_{t+1}^2 &= \mathcal{S}(\varepsilon_{t+1}; \sigma_t^2) = (1 - \phi_\sigma) \mu_\sigma - \nu_\sigma + (\phi_\sigma - \nu_\sigma \beta_\sigma^2) \sigma_t^2 + \nu_\sigma (\varepsilon_{t+1} - \beta_\sigma \sigma_t)^2,\end{aligned}\tag{17}$$

where μ_σ denotes the unconditional mean of volatility, $0 < \phi_\sigma < 1$ modulates the persistence of macroeconomic uncertainty, β_σ determines the correlation between consumption growth and innovations in consumption volatility, and ν_σ is the volatility of volatility parameter. The unconditional variance of σ_t^2 is given by:

$$\sigma_\sigma^2 = \frac{2\nu_\sigma^2 (1 + 2\beta_\sigma^2 \mu_\sigma)}{1 - \phi_\sigma^2},\tag{18}$$

and the volatility process is well defined if we impose the restrictions $(1 - \phi_\sigma) \mu_\sigma - \nu_\sigma \geq 0$ and $\phi_\sigma - \nu_\sigma \beta_\sigma^2 \geq 0$. Given μ_σ , $0 < \phi_\sigma < 1$ and σ_σ , these two non-negativity constraints imply that the volatility of volatility ν_σ and the leverage coefficient β_σ are given by:

$$\nu_\sigma = \sqrt{\frac{(1 - \phi_\sigma^2) \sigma_\sigma^2}{2(1 + 2\beta_\sigma^2 \mu_\sigma)}} \quad \text{and} \quad \beta_\sigma^{\min} \leq |\beta_\sigma| \leq \beta_\sigma^{\max},$$

⁵An exponential GARCH model (Nelson; 1991) for consumption growth volatility would also keep solutions bound to a single integration if consumption growth is driven by a single shock. Tédongap (2015) uses such dynamics to study the implications of economic uncertainty for the cross-section of stock returns.

where

$$\beta_{\sigma}^{\min} = \sqrt{\max\left(0, \frac{1}{2\mu_{\sigma}} \left(\frac{1}{2} \frac{1 + \phi_{\sigma}}{1 - \phi_{\sigma}} \frac{\sigma_{\sigma}^2}{\mu_{\sigma}^2} - 1\right)\right)}$$

$$\beta_{\sigma}^{\max} = \sqrt{\frac{2\phi_{\sigma}^2\mu_{\sigma} + \sqrt{2\phi_{\sigma}^2(2\phi_{\sigma}^2\mu_{\sigma}^2 + (1 - \phi_{\sigma}^2)\sigma_{\sigma}^2)}}{(1 - \phi_{\sigma}^2)\sigma_{\sigma}^2}}.$$

If $\beta_{\sigma} > 0$, then the two innovations are negatively correlated; they are positively correlated if $\beta_{\sigma} < 0$, and they are uncorrelated if $\beta_{\sigma} = 0$. The calibration of the model therefore requires a choice on the value of the leverage parameter β_{σ} . Note that the leverage coefficient introduces skewness in multi-period consumption growth rates, even though there is no skewness at the monthly horizon.

For the analysis of nominal prices, we specify a process for inflation that is qualitatively similar to inflation dynamics proposed in Wachter (2005) or Piazzesi and Schneider (2006), for example. More precisely, we assume that growth rates in prices have a time-varying mean and volatility. The dynamics of inflation π_{t+1} depend on the state vector $\mathbf{Y}_{t+1} = [z_{t+1}, v_{t+1}]^{\top}$, where the two states variables are expected inflation, z_{t+1} , and price growth residual uncertainty, v_{t+1} , which impacts both expected and realized inflation as follows:

$$\begin{aligned}\pi_{t+1} &= \mu_{\pi} + z_t + (\nu_{\pi}\sigma_t\varepsilon_{t+1} + \sqrt{v_t}\eta_{t+1}) \\ z_{t+1} &= \phi_z z_t + \nu_z (\nu_{\pi}\sigma_t\varepsilon_{t+1} + \sqrt{v_t}\eta_{t+1}), \\ v_{t+1} &= (1 - \phi_v)\mu_v - \nu_v + (\phi_v - \nu_v\beta_v^2)v_t + \nu_v(\eta_{t+1} - \beta_v\sqrt{v_t})^2,\end{aligned}\tag{19}$$

where η_{t+1} is an independent and identically distributed standard normal shock, orthogonal to the shocks in consumption growth ε_{t+1} . The affine dynamics for inflation uncertainty ensure that the numerical solution remains restricted to a one-dimensional integration.

The inflation dynamics imply that innovations in expected and realized inflation are perfectly positively correlated, and shocks to aggregate consumption growth impact both expected and realized inflation. The parameter μ_{π} denotes the average inflation rate, $0 <$

$\phi_z < 1$ modulates the persistence of expected price growth, ν_z scales the level of expected inflation volatility, and ν_π determines how uncertainty about real growth affects both realized and expected inflation. A negative value for ν_π imposes a negative correlation between innovations in consumption growth and innovations in realized and expected inflation.

The volatility process v_t is assumed to be the residual component of inflation volatility that is orthogonal to consumption volatility. The above specification suggests that, similar to the volatility of aggregate consumption growth, v_t follows a GARCH recursion with similar parameter restrictions to ensure its positivity. The persistence of residual inflation uncertainty is parametrized through ϕ_v , μ_v defines the average level of residual inflation volatility and ν_v governs the volatility of volatility. The parameter β_v is a leverage coefficient, governing the correlation between inflation volatility innovations and both expected and realized price growth. The leverage parameter introduces skewness in low-frequency price growth, even though inflation has zero skewness at the single-period (monthly) horizon. Thus quarterly and yearly inflation rates are skewed. We note that these dynamics can be mapped into the general framework defined in Equation (14) as follows:

$$\begin{aligned}
A(a, b, \sigma_t^2, \varepsilon_{t+1}) &= a\mu_\pi + b_2((1 - \phi_v)\mu_v - \nu_v) - \frac{1}{2} \ln(1 - 2b_2\nu_v) + (a + b_1\nu_z)\nu_\pi\sigma_t\varepsilon_{t+1} \\
H_1^\$(a, b) &= a + b_1\phi_z \\
H_2^\$(a, b) &= b_2\phi_v + \frac{(a + b_1\nu_z - 2b_2\nu_v\beta_v)^2}{2(1 - 2b_2\nu_v)}.
\end{aligned} \tag{20}$$

Note that our model features inflation-neutrality as in Wachter (2005), Piazzesi and Schneider (2006), and Koijen et al. (2010), among others. This contrasts with Bansal and Shaliastovich (2013), who allow expected inflation to negatively affect future growth.⁶ We allow innovations in consumption growth to correlate with both realized and expected in-

⁶Non-neutrality of inflation is motivated by a negative empirical relation between expected growth and lagged inflation forecasts, although the relation is insignificantly estimated. The working paper version of Bansal and Shaliastovich (2013) likewise features inflation neutrality and sensitivity of expected and realized inflation to innovations in consumption growth.

flation. Given $\nu_\pi < 0$, we obtain a negative correlation between consumption growth and inflation at multiple leads, which is an important feature of the data, as highlighted in Figure 1 of Piazzesi and Schneider (2006).

Given the explicit dynamics for aggregate consumption growth, the price of the real zero-coupon bond depends on a single state variable, the volatility of aggregate consumption growth. In contrast to real bonds, the price of a nominal zero-coupon bond $P_{n,t}^\$$ also depends on expected inflation and inflation uncertainty. Using the law of iterated expectations and conditioning on the realizations of innovations to consumption growth, we keep the numerical solution restricted to a one-dimensional integration. Taken the inflation dynamics as given, nominal bond prices are equal to:

$$P_{n,t}^\$ = P_n^\$(\sigma_t^2) \exp(B_{z,n}^\$ z_t + B_{v,n}^\$ v_t), \quad (21)$$

where the coefficients $B_{z,n}^\$$ and $B_{v,n}^\$$ satisfy the recursions

$$\begin{aligned} B_{z,n}^\$ &= \phi_z B_{z,n-1}^\$ - 1 \\ B_{v,n}^\$ &= \phi_v B_{v,n-1}^\$ + \frac{(\nu_z B_{z,n-1}^\$ - 2\nu_v \beta_v B_{v,n-1}^\$ - 1)^2}{2(1 - 2\nu_v B_{v,n-1}^\$)}, \end{aligned} \quad (22)$$

with initial conditions $B_{z,0}^\$ = 0$ and $B_{v,0}^\$ = 0$. The sequence $\{P_n^\$(\sigma_t^2)\}$ satisfies the recursion

$$P_n^\$(\sigma_t^2) = E_t [M_{t,t+1} P_{n-1}^\$(\sigma_{t+1}^2) \exp(A(-1, B_{n-1}^\$, \sigma_t^2, \varepsilon_{t+1}))], \quad (23)$$

with initial condition $P_0^\$(\sigma_t^2) = 1$, and where $B_{n-1}^\$$ denotes the two-dimensional vector with components $B_{z,n-1}^\$$ and $B_{v,n-1}^\$$. The recursion in Equation (23) has no closed-form solution and is solved by one-dimensional numerical integration over a grid of values for σ_t^2 .

3.3 Calibration and Data

In the column labeled “GDA1” of Table 1, we summarize the calibration of our benchmark model, which is consistent with standard calibrations in long run risk models, such as Bansal et al. (2012) or Bonomo et al. (2011). We calibrate the affine GARCH dynamics in Equation (17) at the monthly decision interval to match the first and second moments of real annual U.S. consumption growth from 1929 to 2018. The mean of consumption growth is calibrated to $\mu_c = 0.0015$. The unconditional volatility of consumption growth, which is equal to $\sqrt{\mu_\sigma}$, is defined to be $\sqrt{\mu_\sigma} = 0.7305 \times 10^{-2}$. We set the persistence and the volatility of consumption volatility to $\phi_\sigma = 0.995$ and $\sigma_\sigma = 0.7546 \times 10^{-4}$. Given μ_σ , ϕ_σ and σ_σ , we choose $\beta_\sigma = \beta_\sigma^{\min}$ and ν_σ is defined in terms of the other parameter values.

The mean inflation level μ_π is equal to 0.0030 and the inflation leverage on news ν_π is -0.1294, implying that realized and expected inflation are negatively correlated with innovations in consumption growth. The negative correlation between consumption growth and both contemporaneous and expected inflation is an important feature of the data (Piazzesi and Schneider; 2006) necessary to generate an upward term structure of nominal yields. Recursive utility is helpful in generating greater risk premia for long-maturity bonds, as the negative correlation between innovations in consumption growth and expected inflation imply that the real payoffs from nominal bonds are low when consumption growth is low. This effectively means that nominal bonds do not provide a good hedge against periods of low consumption growth. Investors, therefore, demand a premium for holding long-term bonds.

Expected inflation is highly persistent with a value of $\phi_z = 0.9840$ and the sensitivity of expected inflation to realized inflation shocks is $\nu_z = 0.3457$. The average inflation uncertainty parameter is equal to $\mu_v = 6.3698 \times 10^{-7}$ and the persistence of inflation volatility is $\phi_v = 0.85$. Finally, we calibrate the volatility parameter of the residual inflation volatility to $\nu_v = 9.5546 \times 10^{-8}$ and the leverage coefficient is given by $\beta_v = -2.9827 \times 10^{-3}$. Thus, inflation volatility is positively correlated with expected and realized price growth, which

also implies positive low-frequency inflation skewness.

Regarding preferences, we calibrate the intertemporal elasticity of substitution ψ at 1.5 and the constant relative risk aversion parameter γ at 2. This parameter configuration implies a preference for early resolution of uncertainty, as is suggested empirically by the estimations in Bansal and Shaliastovich (2013) and Augustin and Tédongap (2016), among others. The disappointment aversion parameter ℓ is fixed at 1 and we set the threshold of the certainty equivalent below which outcomes become disappointing, κ , equal to 0.95. Thus, in our benchmark calibration, any outcome that is more than 5% below the certainty equivalent will be considered disappointing and will lead to a reshuffling of the state price probabilities. The subjective discount factor δ is equal to 0.9985.

We define a benchmark grid of 501 points for σ_t^2 , and we later evaluate the numerical precision of the solutions for alternative grid scenarios. The grid is defined in terms of the natural logarithm of σ_t^2 , which has approximately a mean of $\mu_h = \ln \mu_\sigma - \sigma_h^2/2$ and a standard deviation of $\sigma_h = \ln(1 + \sigma_\sigma^2/\mu_\sigma^2)$.⁷ We use 334 logarithmically spaced points between $\mu_h - 7\sigma_h$ and μ_h , and 167 logarithmically spaced points between μ_h and $\mu_h + 5\sigma_h$. The lower segment is finer and includes values for volatility that are much closer to zero. This better captures the non-linear behavior of the welfare valuation ratio as volatility approaches zero. Given the assumed dynamics, more than 99.9% of the population distribution of $\ln \sigma_t^2$ lies between seven standard deviations below and five standard deviations above the mean. We choose the adaptive Simpson quadrature method as the numerical integration routine.

To evaluate the implications of the model, we simulate a time series of 300,000 months of data and compare the population moments to the sample data.⁸ We use real data sampled at an annual frequency over the period 1929 to 2018. Data for consumption and price growth are taken from the Bureau of Economic Analysis National Income and Product Accounts

⁷More precisely, μ_h and σ_h are approximate solutions to the mean and standard deviation of the logarithm of σ_t^2 when we apply a log-normal approximation to the volatility dynamics and if we ignore skewness. We emphasize that we obtain a grid for σ_t^2 by taking the exponent of the grid on $\ln \sigma_t^2$ element-by-element.

⁸A simulation of 300,000 monthly observations is equivalent to the simulation of 100,000 quarters in Wachter (2005). In all simulations, we use a burn-in period of equal size, i.e. 300,000 months of data.

tables. To compare the model’s solutions to the term structure of nominal interest rates, we use monthly Fama-Bliss discount bond prices from the CRSP U.S. Treasury Database from January 1964 through December 2018. Fama-Bliss Discount Bond Files contain artificial discount bonds with 1 to 5 years to maturity, constructed after first extracting the term structure from a filtered subset of the available bonds. This database is a refinement of the one used in Fama and Bliss (1987).

4 Model Solutions and Analysis

We first discuss the ability of the model calibration to match actual moments of real and nominal growth in Section 4.1. Next, in Section 4.2, we discuss the numerical solution to the welfare valuation ratios. We then report in Section 4.3 the results for the term structure of nominal interest rates. We discuss the model’s mechanism in Section 4.4. We end by studying bond market predictability in Section 4.5.

4.1 Real and Nominal Growth

In Panel A of Table 2, we compare the time-averaged annual moments, computed from a simulated series of 300,000 monthly observations, to the observed sample moments, estimated using annual data from 1929 to 2018. Focusing first on the dynamics of consumption growth, there is a close fit between the (statistically significant) estimated and the model-implied unconditional moments. The mean growth rate is 1.94% in the data, while it is 1.79% in the model. Similarly, the comparison of the volatilities of consumption growth indicates 1.93% in the data versus a model-implied value of 2.08%. We obtain an annualized first-order auto-correlation of 0.24, which is a bit lower than the estimated value of 0.47. This is expected, as we specify monthly consumption growth to be unpredictable.⁹ Finally, we

⁹We provide in Section 5 an extension of the model with predictable consumption growth, allowing for a higher first-order auto-correlation coefficient.

also obtain a reasonable fit for the skewness and kurtosis of the aggregate consumption growth dynamics.¹⁰ Overall, the dynamics we have chosen for our empirical application closely reflect the distribution of aggregate consumption growth, as all values are within two standard deviations of the sample estimates.

In Panel B of Table 2, we provide similar statistics for the shorter post-war period from 1947 to 2018. One key difference is that the volatility of consumption growth estimated at 1.19% is significantly lower in the post-war period than the 1.93% reported in the long sample. A second major difference is that excluding the second World War leads to estimates of consumption growth that are significantly less leptokurtic. Most other target moments remain largely unchanged. In Panels A to C of Appendix Table A.1, we further split the evidence into the periods before and after the Federal Reserve’s “monetarist experiment” of 1979–1982, and the decade following the Global Financial Crisis in 2008. These sample splits suggest that real uncertainty dropped to even lower levels in the period after 1981.

On the right-hand side of Panel A in Table 2, we compare the model-implied population values of the inflation process to the data estimates. Expected inflation is 3.00% (3.57%) in the sample (model), the annualized volatility is 3.20% (2.89%), the first-order auto-correlation coefficient is 0.83 (0.86), and the kurtosis is 8.73 (6.15). The skewness of inflation is estimated negatively at -0.66, although the estimate is not statistically different from zero. The model-implied value for inflation skewness is 1.34. This result arises because of the negative leverage parameter β_v in the inflation volatility dynamics, and is consistent with those authors who argue for positive skewness in inflation (e.g., Aizenman and Hausmann (1994), Chaudhuri et al. (2013), and references therein). However, the estimates reported in Panel B of Table 2 indicate that inflation skewness is positive and equal to 1.39 in the post-war period, and inflation is also less volatile with a standard deviation of 2.26%. Panels A to B of Appendix Table A.1 indicate that the unconditional mean of inflation is

¹⁰The time aggregation introduces skewness at the annual horizon because of the leverage effect, even though the non-predictable consumption growth dynamics have zero skewness at the monthly horizon.

3.71% between 1947 and 1981, while it drops to 2.23% in the years between 1982 and 2018.

4.2 Welfare Valuation Ratios

We next discuss the numerical solution to the utility-consumption ratio. A solution to this welfare valuation ratio is the primary input to solutions for the stochastic discount factor, and therefore for asset prices. In Figure 1a, we plot the welfare valuation ratio $V_t/C_t = G^V(\sigma_t^2)$ as a function of consumption volatility σ_t^2 for our benchmark scenario with 501 grid points. The negative slope suggests that the ratio of utility to the level of consumption is decreasing for higher levels of consumption volatility. This is consistent with the view that agents dislike macroeconomic uncertainty. To shed some light on the robustness of the numerical solution, we evaluate the solution to the welfare valuation ratio for different grids. We specify different densities ranging from the coarsest grid with 24 points to the finest grid with 750 points. We plot in Figure 1b the welfare valuation ratio $V_t/C_t = G^V(\sigma_t^2)$ as a function of consumption volatility for each of these grids. There is a significant difference in the results between the solution derived from the coarsest grid with 24 points and the one with 75 points. The difference in solutions based on the grids with 75 and 123 points is substantially smaller. There is hardly any improvement for the solution using 750 grid points over the solution using a grid of 498 points. This suggests that the solution is accurate and that increasing the number of grid points beyond 501 points is unnecessary.

Another statistic of interest in models with (generalized) disappointment aversion is the disappointment probability. In Figure 1c, we report the probability of disappointment $\xi(\sigma_t^2)$ as a function of consumption volatility σ_t^2 . Without macroeconomic uncertainty, it is unlikely that the agent is disappointed (i.e., probability close to zero percent) as there is little probability of falling below the certainty equivalent threshold. As consumption volatility increases, the disappointment probability increases as well. It equals approximately 8% when the level of the monthly consumption growth volatility equals $\sigma_t = 1\%$.

We further evaluate the precision of the numerical solution by focusing on Epstein and Zin (1989) recursive utility without disappointment version. For that model, we can derive closed-form solutions and compare them to numerical solutions obtained using the same method described above. The Epstein and Zin (1989) model is nested in the model with disappointment and easily obtained by setting the disappointment intensity to zero, i.e., $\ell = 0$, and by relying on the Campbell and Shiller (1988a) log-linearization of returns. Details of the analytical solutions are reported in Appendix C. In Figure 1d, we plot the welfare valuation ratio $V_t/C_t = G^V(\sigma_t^2)$ as a function of consumption volatility σ_t^2 for both the analytical (dotted line) and the numerical (solid line) solution for our benchmark scenario with 501 grid points. The consumption growth parameters are identical to those for the model GDA1 reported in Table 1. The preference parameters for this example are $\delta = 0.9989$, $\psi = 1$, and $\gamma = 4$. We recall that the analytical log-linear solution is exact when $\psi = 1$. The graph visually illustrates that the numerical solution is accurate. There is a slight discrepancy between the two lines, reflecting the numerical precision of the solution method. Quantitatively, the relative root mean squared error is equal to 1.56%, with a maximum of 1.59% when the volatility is close to zero.

4.3 The Term Structure of Real and Nominal Interest Rates

We plot in Figure 2a the real yields $y_{n,t}$ as a function of consumption volatility for maturities of one ($n = 1$) to five ($n = 5$) years. The model implies a downward sloping term structure of real interest rates. This is consistent with the intuition that inflation-indexed bonds represent a valuable hedge for long-term investors, which are willing to pay a premium to hold such assets (Campbell et al.; 2009). Payoffs of real bonds are fixed in consumption units, which are more highly valued when macroeconomic uncertainty is high. As real bond returns are negatively correlated with the level of consumption and stock prices, they command a negative risk premium that increases with the asset horizon. This channel is particularly

true if shocks to macroeconomic uncertainty are persistent. In that case, positive innovations in economic uncertainty can lead to extended periods of slow growth, which increases real bond prices in recessions. A negative slope of the real yield curve is also consistent with a negative term structure of real interest rates found in the long-term U.K. data (Evans; 1998). For very high levels of macroeconomic uncertainty, the slope of the term structure of real interest rates becomes slightly more negative, as can be seen through the wider dispersion in the yields as we move closer to the right of the figure. At very high levels of consumption volatility (and for long horizons), real yields become negative. This is a common feature of recursive utility models with long run risks when the parameter calibration implies a preference for early resolution of uncertainty (Bansal and Shaliastovich; 2013).

We next turn to the term structure of nominal interest rates. In Panel A of Table 3, we report the model-implied term structure of nominal yields and the corresponding volatilities from the simulation with 300,000 months of data, corresponding to 25,000 years. The one-year and the five-year nominal yields are 5.16% and 5.86%, compared to the values of 5.16% and 5.84% in the data, which are reported in Panel B. Thus, we match both the level and the slope of the term structure well. The volatility of nominal bond yields is a bit lower than in the data, but we match the downward sloping pattern. In Panel A of Appendix Table A.2, we report the model’s implications for the term structure of nominal interest rates when the dynamics of consumption growth are calibrated to match the shorter post-war sample, in which the volatility of consumption growth is lower, as we document in Panel B of Table 2. While the model still delivers a close fit for the yield levels, with values ranging from 5.14% at the 1-year to 5.87% at the 5-year horizon, the level of volatilities is sharply reduced to a value of 0.83% at the 1-year maturity compared to 3.33% observed empirically.

In Panels C to E of Table 3, we report the term structure of yield levels and volatilities for the periods before and after the Fed’s monetarist experiment, and the decade after the Global Financial Crisis. The level of yields was significantly higher in the period that includes the inflationary episode of the 70s, with a one-year yield equal to 6.99%. The term structure

was also flatter, as the 5-year yield of 7.11% implies a term spread of only 12 basis points. The decade since the financial crisis has witnessed demonstrably lower levels and volatilities of nominal rates.

4.4 A Discussion of the Model Mechanism

Equation (21) highlights that nominal bond prices are non-linear functions of three sources of risk: macroeconomic uncertainty, expected inflation, and residual inflation uncertainty. To sharpen the intuition about the model's mechanism, we first plot in Figures 2b and 2c the sensitivities of nominal bond yields $y_{n,t}^{\$}$ to expected inflation ($-B_{z,n}^{\$}/n$) and inflation volatility ($-B_{v,n}^{\$}/n$), as these maturity-dependent coefficients are known in closed form.¹¹ The loading of nominal bond yields to expected inflation is positive, implying that high expected inflation raises risk premia and increases nominal yield spreads. Because nominal bond payoffs are fixed in terms of price levels, their returns (prices) are high (low) when expectations about future price growth are high. Innovations in consumption growth are negatively correlated with both realized and expected inflation. In other words, high expected inflation reflects a negative innovation to consumption growth. Thus, investors will issue bonds to borrow from future consumption. This depresses nominal bond prices and raises nominal yields. Since the loadings $-B_{z,n}^{\$}/n$ are negative functions of the asset horizon, short-run yields are comparatively more sensitive to expected inflation shocks than longer-term yields.

The loadings of nominal bond yields to inflation uncertainty are negative at all maturities. Thus, inflation volatility lowers nominal bond yields, which reflects a flight-to-quality effect across all asset horizons. In times of high nominal uncertainty, investors develop a precautionary savings motive. This leads them to buy nominal bonds, which raises their prices and lowers nominal yields. Given that $-B_{v,n}^{\$}/n$ is negative and has a negative slope too, the reduction in yields is comparatively greater at longer horizons than at short-term

¹¹Since $y_{n,t}^{\$} = -n^{-1}p_{n,t}^{\$}$, we have that $y_{n,t}^{\$} = -n^{-1}(p_n^{\$}(\sigma_t^2) + B_{z,n}^{\$}z_t + B_{v,n}^{\$}v_t)$.

maturities. Expected inflation and inflation uncertainty thus have opposing effects on the level of nominal interest rates, even though increases in both risk factors are associated with a more attenuated slope of their term structure.

The third source of risk that impacts nominal bond yields is real uncertainty. As Equation (21) shows, we cannot study the sensitivity of nominal bond yields to real uncertainty independently from expected price growth and inflation uncertainty. To investigate the sensitivity of nominal bond yields to consumption volatility, we thus fix the values of expected inflation and inflation uncertainty at their long run average values. Conditional on these values, we plot in Figure 2d nominal bond yields for maturities of one to five years as a function of consumption volatility. All nominal yields are lower for higher levels of real uncertainty. This reflects a flight-to-quality effect, whereby bond prices (yields) respond positively (negatively) to macroeconomic uncertainty. Figure 2d also illustrates that short-term nominal yields are more sensitive to economic uncertainty than long-term nominal yields. This is characterized by the differences in the steepness of each maturity line plot. Thus, in contrast to nominal uncertainty, higher real uncertainty is associated with a steeper slope of the term structure of interest rates.

To summarize, in a simple economy with three sources of risk – expected inflation and both real and inflation uncertainty – and preferences that include disappointment aversion, we generate an upward sloping term structure of nominal bond yields. Yields rise in response to shocks to expected inflation and decrease in response to shocks to inflation and economic uncertainty. Thus, the flight-to-quality effect dominates the intertemporal substitution effect for the response of nominal yields to a rise in real and nominal uncertainty. We generate an upward sloping term structure of nominal bond yields without shocks to expected growth as in Bansal and Shaliastovich (2013). At the same time, we generate countercyclical real interest rates, in contrast to an upward sloping term structure of real interest rates as in Wachter (2005). The success of the model is partly due to the ability of the GDA preferences to generate variation in the pricing kernel that is much larger than what is obtained in

standard recursive utility with symmetric preferences. To see this, we use Equation (6) to express the conditional variance of the log stochastic discount factor, $m_{t,t+1} = \ln M_{t,t+1}$, as:

$$\begin{aligned} Var_t[m_{t,t+1}] &= Var_t[m_{t,t+1}^*] + (\ln(1 + \ell))^2 Var_t[I(V_{t+1} < \kappa \mathcal{R}_t(V_{t+1}))] \\ &\quad + 2 \ln(1 + \ell) Cov_t(m_{t,t+1}^*, I(V_{t+1} < \kappa \mathcal{R}_t(V_{t+1}))), \end{aligned} \quad (24)$$

where $Var_t[m_{t,t+1}^*]$ represents the conditional variance of the pricing kernel with Epstein and Zin (1989) recursive utility. The two additional terms are strictly non-negative. As a consequence, the conditional variance of the log pricing kernel with GDA preferences is always at least as large as that of an equivalent pricing kernel without GDA. This feature is a useful ingredient to solve asset pricing puzzles such as the equity premium and the risk-free rate puzzles of Mehra and Prescott (1985) and Weil (1989), respectively, as shown by Bonomo et al. (2011). Another merit of the framework with asymmetric preferences is that state probabilities are reshuffled if an outcome is below a fraction κ of the certainty equivalent. Through this mechanism, the model endogenously generates effective countercyclical risk aversion. This property is useful to explain stylized predictability patterns in stock and bond markets. In that regard, we exploit in Section 4.5 the simulated time series of nominal bond yields to show that the model also accounts for the failure of the expectations hypothesis.

One of the advantages of the model with disappointment aversion is that it allows us to examine how asset prices respond in-sample to the endogenously time-varying disappointment probability. We, therefore, plot in Figure 3 the filtered disappointment probability for our sample period. The disappointment probability is a function of the consumption growth volatility described in Equation (17). Hence, we overlay in Figure 3a the filtered time series of real uncertainty, which we impute from monthly real per capita consumption growth data using the calibrated parameters of our benchmark consumption dynamics (Model GDA1 in Table 1). Both the disappointment probability and the consumption growth volatility are strongly positively correlated and tend to increase during NBER recessions.

In Figure 3b, we plot the disappointment probability together with the 1-year nominal yield. While there is no clear relation in the early part of the sample, we observe a strong negative relation in the period following the Fed’s monetarist experiment. The short-term interest rate is lower in times of high disappointment. In Figure 3c, we overlay the term spread, which increases in response to more disappointment. This is because even though the higher disappointment driven by higher real uncertainty lowers nominal yields, it has a greater impact on short-term interest rates, thereby steepening the term structure. Finally, we illustrate in Figure 3d the relation between disappointment and the five-year risk bond premium estimated using the Cochrane and Piazzesi (2005) risk premium factor that is constructed from the cross-section of forward rates. There is no clearly visible relation between the two series, which is expected, as risk premiums are determined by both real and nominal uncertainty.

4.5 Predictability and the Expectations Hypothesis

The empirical failure of the expectations hypothesis of interest rates, documented by Fama and Bliss (1987) and Campbell and Shiller (1991), has motivated the development of economic models seeking to explain that puzzle. Backus et al. (1989) show that the standard Consumption Capital Asset Pricing Model with power utility cannot account for the anomaly. Recent theoretical explanations that have been suggested use the long run risk framework of Bansal and Yaron (2004) or the external habit setup of Campbell and Cochrane (1999). Wachter (2006) uses external habits with countercyclical interest rates to generate an upward sloping term structure of nominal bonds and predictability in bond returns. An alternative setup with habit preferences has been suggested by Le et al. (2010). In contrast, Bansal and Shaliastovich (2013) suggest that time-varying expected growth rates, expected inflation, and real and inflation uncertainty, together with Epstein and Zin (1989) recursive utility and preference for early resolution of uncertainty, yield time-varying bond risk premia and

an upward sloping term structure of interest rates.¹² Our model, which generates an upward sloping term structure of nominal bonds, also reproduces predictability patterns in bond returns that are quantitatively close to the standard tests of the expectations hypothesis. We achieve these results without predictability in consumption growth.

The expectations hypothesis predicts that excess bond returns are unpredictable and that risk premia are constant. Various tests of the theory yield the same conclusion that there is significant evidence of predictability in bond returns, suggesting the presence of time-varying risk premia. We evaluate the success of our model by its ability to reproduce the multiplicity of empirical regression results suggested over the last decade. For instance, Fama and Bliss (1987) project holding period returns on the corresponding forward-spot spread:

$$rx_{n,t+12} = \alpha_n + \beta_n (f_{n,t} - y_{1,t}^{\$}) + \varepsilon_{n,t+12}, \quad (25)$$

where $rx_{n,t+12}$ indicates the annual excess log return of a n -year bond over the one-year yield $y_{1,t}^{\$}$ defined as $rx_{n,t+12} = r_{n,t+12} - y_{1,t}^{\$}$, with the return given by the difference in log prices, that is $r_{n,t+12} = p_{n-1,t+12}^{\$} - p_{n,t}^{\$}$. We recall that all t subscripts refer to a monthly sampling frequency, while all n subscripts refer to the bond maturity in years. The forward spread $f_{n,t}$ for a loan between time $t + 12(n - 1)$ and time $t + 12n$ is defined as $f_{n,t} = p_{n-1,t}^{\$} - p_{n,t}^{\$}$. Alternatively, Campbell and Shiller (1991) regress changes in long yields on the yield spread as follows:

$$y_{n-1,t+12}^{\$} - y_{n,t}^{\$} = \alpha_n + \beta_n \frac{1}{n-1} (y_{n,t}^{\$} - y_{1,t}^{\$}) + \varepsilon_{n,t+12}. \quad (26)$$

All these regressions predict a slope coefficient of one, an outcome that is strongly rejected in the data. Dai and Singleton (2002) suggest that adding the bond risk premium to the left-hand side of the regression can restore the unity regression coefficient. Thus, a model that is able to bring the slope coefficient closer to its predicted value should help resolve the

¹²While these are the most recent articles on the topic, other relevant references are Bekaert et al. (1997), Longstaff (2000), Bekaert and Hodrick (2001), Bansal and Zhou (2002), Dai and Singleton (2002) and Buraschi and Jiltsov (2005).

expectations hypothesis puzzle. We also test our model on their adjusted regression model:

$$y_{n-1,t+12}^{\$} - y_{n,t}^{\$} + \frac{1}{n-1} \hat{E}_t [r_{n,t+12} - y_{1,t}^{\$}] = \alpha_n + \beta_n \frac{1}{n-1} (y_{n,t}^{\$} - y_{1,t}^{\$}) + \varepsilon_{n,t+12}, \quad (27)$$

where $\hat{E}_t [r_{n,t+12} - y_{1,t}^{\$}]$ defines the risk premium component of nominal bond yields. Our last test is based on the results of Cochrane and Piazzesi (2005), who show that a single factor projection based on one-year to five-year forward rates captures a significant variation in bond returns. The CP factor is obtained in a two-step estimation procedure, whereby first the average of one-year excess bond returns of two to five years to maturity are regressed on one to five year forward rates, $\frac{1}{4} \sum_{n=2}^5 rx_{n,t+12} = \gamma_{n,0} + \gamma_{n,1}y_{1,t}^{\$} + \gamma_{n,2}f_{2,t} + \dots + \gamma_{n,5}f_{5,t} + \varepsilon_{n,t+12}$. The fitted value of that regression is the CP_t bond factor, which is then used in a second step to forecast excess bond returns at each maturity from two to five years:

$$rx_{n,t+12} = \beta_n CP_t + \varepsilon_{n,t+12}. \quad (28)$$

We report in Table 4 the results of the model-implied predictability regressions and compare them to the data. We start with the description of the Cochrane-Piazzesi restricted single factor regressions in Panel A of Table 4. There is a close match between both the regression coefficients and the R^2 of the regressions. The model-implied slope coefficients range from 0.42 to 1.56 for the two- and five-year maturities, compared with a range of 0.45 to 1.46 in the data. The model-implied standard errors are significantly smaller, which is due to the regressions with 300,000 observations; the observed sample has 660 data points. In addition, over the sample period 1964 to 2018, the single factor forecasts excess bond returns with an R^2 statistic of 20% at the 2-year horizon. Predictability increases up to 4 years with an R^2 of 25% and flattens out a bit with a value of 23% for 5-year bonds. The model-implied statistics range from 19% at the 2-year horizon to 20% at the 5-year maturity.

In Panels B, C, and D of Table 4, we report the model-implied results for the Fama and

Bliss (1987), the Campbell and Shiller (1991), and the Dai and Singleton (2002) regressions, respectively. We compare all model-implied results to the observed counterparts, estimated in the data using prices from 1964 to 2018. Overall, we confirm the previous evidence of predictability of excess bond returns by bond yields. The implied statistics are quantitatively close to the data counterparts, both in terms of regression coefficients and explanatory power. In the Campbell and Shiller (1991) regressions, the beta coefficients for longer maturities are less negative than in the data. In unreported results, we have verified that this is easily adjustable by increasing the persistence of expected inflation. For the adjusted Dai-Singleton regressions, the beta coefficients are indistinguishable from one. This suggests that the model generates a sizable time-varying risk premium in bond returns that helps explain the failure of the expectations hypothesis for nominal bonds.

In Table A.3, we report the model-implied results when we calibrate consumption growth dynamics to the shorter post-war sample, as described in Panel B of Table 2. In that case, the model fails to provide reasonable predictability patterns for excess bond returns because consumption volatility is too low. For comparability, we also provide in Table A.4 the empirical regression counterparts for different sample splits in the post-war period.

5 Model Extensions and Comparison with Literature

Our model relates most closely to Piazzesi and Schneider (2006) and Bansal and Shaliastovich (2013) (henceforth PS and BS), even though their work features differences regarding the specification of preferences and of the endowment economy. Both studies examine the term structure of nominal interest rates in an Epstein and Zin (1989) recursive utility framework without disappointment aversion. PS examine a model with time-varying expected growth rates and constant volatility of consumption growth and inflation. BS, in contrast, allow for time-varying expected consumption growth and expected inflation, both with time-varying volatilities, while conditional variances of consumption growth and inflation remain constant.

We extend our benchmark model for comparisons with these studies. Specifically, we allow expected consumption growth x_t to be varying over time, such that the endowment economy is characterized by two state variables:

$$\begin{aligned}\Delta c_{t+1} &= \mu_c + x_t + \sigma_t \varepsilon_{t+1} \\ x_{t+1} &= \phi_x x_t + \nu_x \sigma_t \varepsilon_{t+1},\end{aligned}\tag{29}$$

where ϕ_x modulates the persistence of shocks to expected growth, and where ν_x measures the sensitivity of expected growth to consumption shocks. Shocks to realized and expected consumption growth (ε_{t+1}) are perfectly positively correlated, which is necessary as we want to restrict the model solution to a single numerical integration. Equation (29), therefore, features a heteroscedastic ARMA(1,1) consumption growth process. This is slightly different from BS, who introduce orthogonal shocks to expected and realized growth rates.

For better comparison with PS, we present results for a third specification in which we restrict consumption growth to be homoscedastic, i.e., $\sigma_t^2 = \mu_\sigma$. Last, for additional cross-model comparison of asset price moments and predictability in stock markets, we introduce a dividend growth process. As the focus of our paper is on asset pricing implications and predictability in bond markets, we describe the dividend growth process, corresponding asset pricing formulas, and its calibration in Appendix D.

We provide a comparison of the asset pricing implications across all models in Table 5 (see Panel A), and compare model implications for the predictability in bond and stock markets in Table 6. First, we examine how the benchmark model (GDA1) performs when we do not allow for disappointment (EZ1), which is easily achieved by setting the disappointment parameter ℓ equal to zero. To match the level and the slope of the nominal yield curve, we adjust the subjective discount factor to $\delta = 0.9989$, and the coefficient of relative risk aversion to $\gamma = 5$, as reported in Panel B. Compared to BS, who estimate γ to be 20.9, we can lower the value of that coefficient because our dynamics of consumption growth feature

a leverage effect, which causes shocks in volatility to be negatively correlated with shocks in consumption growth. This increases the magnitude of skewness and kurtosis of growth rates, which, in the GDA1 model, is an important feature for the predictability in bond markets. BS estimate a slightly higher value for the EIS of $\psi = 1.81$, compared to our value of 1.5.

By construction, in both models, the implied moments for cash flows are identical (Panel C). The results in Panel D of Table 5 suggest that both models generate realistic first and second moments for prices in bond and stock markets, as well as the log price-dividend ratio, regardless of whether agents have asymmetric preferences or not. What distinguishes these two specifications is the predictability patterns in bond and stock markets. For example, the Cochrane-Piazzesi regressions reported in Panel B of Table 6 suggest that, in the GDA1 model, the CP factor predicts 2-year excess bond returns with an R^2 of 18.84%, compared with a value of 19.89% in the data. In contrast, the EZ1 specification produces a value of 11.08%. At the 5-year horizon, these values increase to 20.02% and 11.19% for the GDA1 and EZ1 models, respectively. For the Fama-Bliss regressions reported in Panel C, the model-implied R^2 values for the model with disappointment aversion are about 3 times as large as those found for the model without disappointment aversion. For the Campbell-Shiller regressions, reported in Panel D, the R^2 values at the 2-year (5-year) horizon are 1.28% and 0.00% (1.92% and 0.00%) respectively, compared to 2.06% and 6.13% in the data.

Such large discrepancies between the GDA1 and EZ1 models highlight that asymmetric preferences together with a high volatility of volatility in consumption growth are important for quantitatively explaining observed patterns of predictability in bond markets. Either one individually is not enough. If we calibrate consumption growth to the post-war sample from 1947 to 2018 (see Panel B of Table 2), consumption growth is less volatile and less leptokurtic. With such dynamics, we still match the level and the slope of the nominal term structure of interest rates, as we show in Table A.2, but our ability to reconcile the observed patterns of predictability in bond markets worsens significantly, as shown in Table A.3.

In Panel E of Table 6, we provide the regression coefficients and R^2 values from regressions

of future excess stock returns on the log price-dividend ratio at the 2-year and 5-year horizons. These results echo those in Bonomo et al. (2011) that a framework with non-predictable consumption growth and disappointment aversion generates large predictability power of future excess stock returns by the dividend-price ratio. Because the dynamics of consumption growth are unpredictable, we further show in Panel F that the log price-dividend ratio has no predictive power for future consumption growth (Beeler and Campbell; 2012).

We next compare model implications for both types of preferences when consumption growth is homoscedastic but has time-varying expected growth, as in PS. We label the model with and without disappointment aversion GDA2 and EZ2, respectively. We slightly adjust the calibration for preferences and cash flows, as described in the column labeled “GDA2” in Table 1. One major difference in terms of cash flows is that there is no negative skewness in consumption growth, and that there is less leptokurtosis in both growth and inflation rates. PS focus on a special case with $\psi = 1$ to obtain closed-form solutions, patient investors, $\delta > 1$, and coefficients of relative risk aversion γ above 40 (59 in their benchmark case). In the EZ2 calibration, we set $\delta = 0.9988$, $\psi = 2$, and $\gamma = 18$ to obtain realistic first and second moments for cash flows, and asset prices in stock and bond markets.

According to Panel D in Table 5, both GDA2 and EZ2 display a term structure of nominal interest rates, and first and second moments for the equity return and the short rate, that match those found in the data. However, the results in Table 6 show a lack of predictability in either the bond or stock markets. Another counterfactual implication observed in Panel F of Table 6 is that the model generates excessive predictability of future consumption growth by the log price-dividend ratio (Beeler and Campbell; 2012, Bansal et al.; 2012).

In a final specification, we allow for both time-varying expected growth and consumption growth volatility. In the column labeled “GDA3” in Table 1, we report values of all the calibrated cash flow and preference parameters for the model with disappointment aversion (GDA3). The version without disappointment aversion (EZ3) compares closely to the model of BS, although they propose time-varying volatility in expected growth rates and inflation,

while their conditional volatilities of consumption growth and inflation are constant. Both models with and without disappointment aversion produce quantitatively realistic results for asset pricing moments and predictability in stock and bond markets. However, the findings in Panel F of Table 6 indicate that such dynamics produce too much predictability of future consumption growth by the log price-dividend ratio, similar to the dynamics with time-varying expected growth rates and homoscedastic consumption growth.

5.1 Discussion and Literature

Gabaix (2012) develops a variable rare disaster model with time separable expected utility and both a real and a nominal disaster shock, each of which has both time-varying intensity and probability of occurrence. While that model generates an upward sloping nominal term structure of interest rates and reconciles the failure of the expectations hypothesis, it produces the counterfactual implication of independent risk premia in stock and bond markets, leading to a lack of cross-asset predictability. Tsai (2016) extends the work of Gabaix (2012) to address these shortcomings in a recursive utility model with variable rare disasters and three state variables that drive risk premia: expected inflation, real disaster shocks and inflation disaster shocks, but with time-varying disaster probabilities. We illustrate similarities and differences across the models most directly related to our work in Appendix Table A.5.

There are other models that study the term structure of nominal interest rates or predictability puzzles in bond markets. However, these models are not directly comparable, as they consider (i) the effect of heterogeneous agents, (ii) a production economy in which the endowments arise endogenously, and (iii) they postulate a monetary economy or a full fledged DSGE model with capital and labor (Buraschi and Jiltsov; 2005, 2007; Ehling et al.; 2018). What all of these models have in common is that they rely on symmetry in preferences, which is inconsistent with the experimental evidence on decision theory. We find it important to understand whether micro-founded macroeconomic models calibrated to be

consistent with asymmetric preferences can match asset prices in the data. For instance, Delikouras (2014) refers to Choi et al. (2007) in the context of portfolio choice problems, who find disappointment aversion coefficients that range from 0 to 1.876 with a mean of 0.390, and second-order risk aversion parameters that range from -0.952 to 2.87 with a mean of 1.448. Similarly, using experimental data on real effort provision, Gill and Prowse (2012) estimate disappointment aversion coefficients ranging from 1.260 to 2.070. See also Artstein-Avidan and Dillenberger (2010) for experimental evidence on disappointment aversion.

In addition, disappointment aversion endogenously produces a time-varying market price of risk, which helps to increase the volatility of the pricing kernel (and therefore helps explain the failure of the expectations hypothesis), without introducing too much predictability of future consumption growth through long run risk in expected growth. There are other ways of *exogenously* imposing a time-varying market price of risk (like learning, or preference shocks), while this feature arises endogenously through preferences with disappointment aversion. Having both a time-varying market price and quantities of risk is an important feature in order to be consistent with the behavior and shape of bond risk premia implied by Gaussian affine term structure models (Creal and Wu; 2020).

6 Conclusion

This paper provides a general framework for preference-based models with generalized disappointment aversion when the economy is modeled to have continuous states. We apply the framework to the term structure of nominal interest rates using a parsimonious model with a single state variable for the real economy, and two state variables for inflation. We model consumption growth as non-predictable with time-varying uncertainty, specified as affine GARCH volatility dynamics. Thus, macroeconomic uncertainty inhibits the same shocks as realized aggregate consumption growth, which has the advantage of restricting the numerical solutions to a single integration. Likewise, we define affine GARCH dynamics for inflation

uncertainty, which impacts both realized and expected inflation.

The key ingredients to the model are disappointment aversion and preference for early resolution of uncertainty. Real bonds depend only on real uncertainty, while nominal bonds also depend on expected inflation and nominal uncertainty. The ability of the model to generate strong countercyclical risk aversion and a high volatility of the pricing kernel enables us to generate an upward (downward) sloping term structure of nominal bond yields (volatilities), consistent with the data. The model also accounts for the failure of the expectations hypothesis. We generate predictability in excess bond returns with substantial time variation in risk premia. Our model-implied regression coefficients are quantitatively close to the sample estimates obtained by most standard tests of the expectations hypothesis.

Investors are disappointed in bad states of the world. This begs the question of whether disappointment aversion improves over other preference frameworks for contingent claims securities that better capture tail events, such as interest rate options. We leave this question for future research.

References

- Aizenman, J. and Hausmann, R. (1994). Why is inflation skewed? A debt and volatility story, *NBER Working Papers 4837*, National Bureau of Economic Research, Inc.
- Artstein-Avidan, S. and Dillenberger, D. (2010). Dynamic disappointment aversion: Don't tell me anything until you know for sure, *PIER Working Paper No. 10-025*.
- Aruoba, S. B., Fernández-Villaverde, J. and Rubio-Ramírez, J. F. (2006). Comparing solution methods for dynamic equilibrium economies, *Journal of Economic Dynamics & Control* **30**(12): 2477–2508.
- Augustin, P. and Tédongap, R. (2016). Real economic shocks and sovereign credit risk, *Journal of Financial and Quantitative Analysis* **51**(2): 541–587.
- Backus, D. K., Gregory, A. W. and Zin, S. E. (1989). Risk premiums in the term structure: Evidence from artificial economies, *Journal of Monetary Economics* **24**(3): 371–399.
- Backus, D. K., Routledge, B. R. and Zin, S. E. (2004). *Exotic Preferences for Macroeconomists*, Vol. 19, MIT Press.

- Bansal, R., Dittmar, R. and Kiku, D. (2009). Cointegration and consumption risks in asset returns, *Review of Financial Studies* **22**(3): 1343–1375.
- Bansal, R., Khatchatrian, V. and Yaron, A. (2005). Interpretable asset markets?, *European Economic Review* **49**(3): 531–560.
- Bansal, R., Kiku, D. and Yaron, A. (2012). An empirical evaluation of the long-run risks model for asset prices, *Critical Finance Review* **1**(1): 183–221.
- Bansal, R. and Shaliastovich, I. (2013). A long-run risks explanation of predictability puzzles in bond and currency markets, *Review of Financial Studies* **26**(1): 1–33.
- Bansal, R. and Yaron, A. (2004). Risks for the long run: A potential resolution of asset pricing puzzles, *The Journal of Finance* **59**(4): 1481–1509.
- Bansal, R. and Zhou, H. (2002). Term structure of interest rates with regime shifts, *The Journal of Finance* **57**(5): 1997–2043.
- Beeler, J. and Campbell, J. Y. (2012). The long-run risks model and aggregate asset prices: An empirical assessment, *Critical Finance Review* **1**(1): 141–182.
- Bekaert, G. and Hodrick, R. J. (2001). Expectations hypotheses tests, *The Journal of Finance* **56**(4): 1357–1394.
- Bekaert, G., Hodrick, R. J. and Marshall, D. A. (1997). On biases in tests of the expectations hypothesis of the term structure of interest rates, *Journal of Financial Economics* **44**(3): 309–348.
- Bloom, N. (2009). The impact of uncertainty shocks, *Econometrica* **77**(3): 623–685.
- Bollerslev, T., Sizova, N. and Tauchen, G. (2012). Volatility in equilibrium: Asymmetries and dynamic dependencies, *Review of Finance* **16**(1): 31–80.
- Bonomo, M., Garcia, R., Meddahi, N. and Tédongap, R. (2011). Generalized disappointment aversion, long-run volatility risk and aggregate asset prices, *Review of Financial Studies* **24**(1): 82–122.
- Buraschi, A. and Jiltsov, A. (2005). Inflation risk premia and the expectations hypothesis, *Journal of Financial Economics* **75**(2): 429–490.
- Buraschi, A. and Jiltsov, A. (2007). Habit formation and macroeconomic models of the term structure of interest rates, *The Journal of Finance* **62**(6): 3009–3063.
- Campanale, C., Castro, R. and Clementi, G. L. (2010). Asset pricing in a production economy with Chew-Dekel preferences, *Review of Economic Dynamics* **13**(2): 379–402.
- Campbell, J. Y. and Cochrane, J. H. (1999). By force of habit: A consumption-based explanation of aggregate stock market behavior, *Journal of Political Economy* **107**(2): 205–251.

- Campbell, J. Y. and Shiller, R. J. (1988a). The dividend-price ratio and expectations of future dividends and discount factors, *Review of Financial Studies* **1**(3): 195–228.
- Campbell, J. Y. and Shiller, R. J. (1988b). Stock prices, earnings, and expected dividends, *The Journal of Finance* **43**(3): 661–676.
- Campbell, J. Y. and Shiller, R. J. (1991). Yield spreads and interest rate movements: A bird’s eye view, *The Review of Economic Studies* **58**(3): 495–514.
- Campbell, J. Y., Shiller, R. J. and Viceira, L. M. (2009). Understanding inflation-indexed bond markets, *Brookings Papers on Economic Activity* pp. 79–120.
- Chaudhuri, K., Greenwood-Nimmo, M., Kim, M. and Shin, Y. (2013). On the asymmetric U-shaped relationship between inflation, inflation uncertainty, and relative price skewness in the UK, *Journal of Money, Credit & Banking* **45**(7): 1431–1449.
- Choi, S., Fisman, R., Gale, D. and Kariv, S. (2007). Consistency and heterogeneity of individual behavior under uncertainty, *American Economic Review* **97**(5): 1921–1938.
- Cochrane, J. H. and Piazzesi, M. (2005). Bond risk premia, *The American Economic Review* **95**(1): 138–160.
- Creal, D. D. and Wu, J. C. (2020). Bond risk premia in consumption-based models, *University of Notre-Dame Working Paper* .
- Dahlquist, M., Farago, A. and Tédongap, R. (2017). Asymmetries and portfolio choice, *Review of Financial Studies* **30**(2): 667–702.
- Dai, Q. and Singleton, K. J. (2002). Expectation puzzles, time-varying risk premia, and affine models of the term structure, *Journal of Financial Economics* **63**(3): 415–441.
- Delikouras, S. (2014). Why corporate bonds may disappoint: Disappointment aversion and the credit spread puzzle, *Working Paper* .
- Delikouras, S. (2017). Where’s the kink? disappointment events in consumption growth and equilibrium asset prices, *Review of Financial Studies* **30**(8): 2851–89.
- Dolmas, J. (2013). Disastrous disappointments: Asset-pricing with disaster risk and disappointment aversion, *Working Paper Federal Reserve Bank of Dallas* .
- Ehling, P., Gallmeyer, M. F., Heyerdahl-Larsen, C. and Philipp (2018). Disagreement about inflation and the yield curve, *Journal of Financial Economics* **127**(3): 459–484.
- Epstein, L. G. and Zin, S. E. (1989). Substitution, risk aversion, and the temporal behavior of consumption and asset returns: A theoretical framework, *Econometrica* **57**(4): 937–969.
- Eraker, B. (2008). Affine general equilibrium models, *Management Science* **54**(12): 2068–2080.

- Evans, M. D. D. (1998). Real rates, expected inflation, and inflation risk premia, *The Journal of Finance* **53**(1): 187–218.
- Fama, E. F. and Bliss, R. R. (1987). The information in long-maturity forward rates, *American Economic Review* **77**(4): 680.
- Farago, A. and Tédongap, R. (2018). Downside risks and the cross-section of asset returns, *Journal of Financial Economics* **129**(1): 69–86.
- Gabaix, X. (2012). Variable rare disasters: An exactly solved framework for ten puzzles in macro-finance, *Quarterly Journal of Economics* **127**(2): 645–700.
- Gill, D. and Prowse, V. (2012). A structural analysis of disappointment aversion in a real effort competition, *American Economic Review* **102**(1): 469–503.
- Gul, F. (1991). A theory of disappointment aversion, *Econometrica* **59**(3): 667–86.
- Hansen, L. P., Heaton, J., Lee, J. and Roussanov, N. (2007). Chapter 61 intertemporal substitution and risk aversion, Vol. 6, Part A of *Handbook of Econometrics*, Elsevier, pp. 3967–4056.
- Heston, S. and Nandi, S. (2000). A closed-form garch option valuation model, *Review of Financial Studies* **13**(3): 585–625.
- Jurado, K., Ludvigson, S. C. and Ng, S. (2015). Measuring uncertainty, *American Economic Review* **105**(3): 1177–1216.
- Kandel, S. and Stambaugh, R. F. (1990). Expectations and volatility of consumption and asset returns, *The Review of Financial Studies* **3**(2): 207–232.
- Koijen, R. S., Lustig, H., Nieuwerburgh, S. V. and Verdelhan, A. (2010). Long run risk, the wealth-consumption ratio, and the temporal pricing of risk, *American Economic Review: Papers & Proceedings* **100**(2): 552–556.
- Kreps, D. M. and Porteus, E. L. (1978). Temporal resolution of uncertainty and dynamic choice theory, *Econometrica* **46**(1): 185–200.
- Le, A. and Singleton, K. J. (2013). The structure of risks in equilibrium affine models of bond yields, *Working Paper*.
- Le, A., Singleton, K. J. and Dai, Q. (2010). Discrete-time affine-Q term structure models with generalized market prices of risk, *Review of Financial Studies* **23**(5): 2184–2227.
- Lettau, M., Ludvigson, S. and Wachter, J. (2008). The declining equity premium: What role does macroeconomic risk play?, *Review of Financial Studies* **21**(4): 1653–1687.
- Longstaff, F. A. (2000). The term structure of very short-term rates: New evidence for the expectations hypothesis, *Journal of Financial Economics* **58**(3): 397–415.

- Marinacci, M. and Montrucchio, L. (2010). Unique solutions for stochastic recursive utilities, *Journal of Economic Theory* **145**(5): 1776–1804.
- Mehra, R. and Prescott, E. C. (1985). The equity premium: A puzzle, *Journal of Monetary Economics* **15**(2): 145–161.
- Nelson, D. B. (1991). Conditional heteroskedasticity in asset returns: A new approach, *Econometrica* **59**(2): 347–70.
- Piazzesi, M. and Schneider, M. (2006). Equilibrium yield curves, *Working Paper 12609*, National Bureau of Economic Research.
- Pohl, W., Schmedders, K. and Wilms, O. (2018). Higher order effects in asset pricing models with long-run risks, *Journal of Finance* **73**(3): 1061–1111.
- Routledge, B. R. and Zin, S. E. (2010). Generalized disappointment aversion and asset prices, *Journal of Finance* **65**(4): 1303–1332.
- Schreindorfer, D. (2019). Macroeconomic tail risks and asset prices, *Review of Financial Studies* **Forthcoming**.
- Stock, J. and Watson, M. (2002). Has the business cycle changed and why?, in *M. Gertler and Kenneth Rogoff, NBER Macroeconomics Annual: 2002, MIT Press Cambridge*.
- Tédongap, R. (2015). Consumption volatility and the cross-section of stock returns, *The Review of Finance* **19**(1): 367–405.
- Timmermann, A. (2000). Moments of markov switching models, *Journal of Econometrics* **96**(1): 75–111.
- Tsai, J. (2016). Rare disasters and the term structure of interest rates, *Working Paper University of Oxford*.
- Wachter, J. A. (2005). Solving models with external habit, *Finance Research Letters* **2**(4): 210–226.
- Wachter, J. A. (2006). A consumption-based model of the term structure of interest rates, *Journal of Financial Economics* **79**(2): 365–399.
- Weil, P. (1989). The equity premium puzzle and the risk-free rate puzzle, *Journal of Monetary Economics* **24**(3): 401–421.

Table 1: Model Parameter Calibration

In this table, we report model and preference parameter values, which are calibrated at a monthly decision interval. Model GDA1 refers to our benchmark model with only volatility in aggregate consumption growth (σ_t). Model GDA2 refers to the model with constant volatility and time-varying expected growth (x_t). Model GDA3 refers to the model with both time-varying expected growth and volatility (x_t, σ_t).

Parameter		GDA1	GDA2	GDA3
		σ_t	x_t	x_t, σ_t
Consumption Growth Dynamics				
Mean consumption growth	μ_c	0.0015	0.0015	0.0015
Persistence of volatility	ϕ_σ	0.9950	–	0.9950
Volatility level	$\sqrt{\mu_\sigma}$	0.0073	0.0048	0.0048
Volatility of volatility	σ_σ	7.546e-5	–	3.258e-5
Persistence of expected consumption growth	ϕ_x	–	0.9750	0.9750
Sensitivity to long-run risk shocks	ν_x	–	0.0380	0.0380
Inflation Dynamics				
Mean inflation rate	μ_π	0.0030	0.0030	0.0030
Persistence of expected inflation	ϕ_z	0.9840	0.9840	0.9840
Inflation leverage on news	ν_π	-0.1294	-0.1509	-0.1509
Level of expected inflation shock volatility	ν_z	0.3457	0.3457	0.3457
Inflation volatility level	μ_v	6.3698e-7	1.0053e-6	1.0053e-6
Persistence of inflation volatility	ϕ_v	0.8500	0.8500	0.8500
Level of residual inflation volatility	ν_v	9.5546e-8	1.5080e-7	1.5080e-7
Inflation volatility leverage coefficient	β_v	-2.9827e+3	-2.374e+3	-2.374e+3
Preference Parameter Values				
Subjective discount factor	δ	0.9985	0.9987	0.9957
Intertemporal elasticity of substitution	ψ	1.5	1.5	∞
Coefficient of relative risk aversion	γ	2.0	2.0	2.0
Coefficient of disappointment aversion	ℓ	1.0	1.0	1.0
Coefficient of generalized disappointment aversion	κ	0.950	0.990	0.971

Table 2: Cash-flows – Annual Data

In this table, we present moments of real per capita consumption and inflation dynamics from the data and the model. The data are real, sampled at an annual frequency, and cover the period 1929 to 2018. Standard errors are Newey-West with one lag. For the model, we report population statistics based on a simulation of 300,000 months. Consumption and price growth rates in the model are time-averaged. Data for consumption and price growth are from the Bureau of Economic Analysis National Income and Product Accounts Tables.

Consumption					Inflation				
Moment	Estimate	SE	T-Stat	Model	Moment	Estimate	SE	T-Stat	Model
Panel A: 1930-2018									
$E[\Delta_c]$ (%)	1.94	0.25	7.70	1.79	$E[\pi]$ (%)	3.00	0.49	6.18	3.57
$\sigma[\Delta_c]$ (%)	1.93	0.37	5.25	2.08	$\sigma[\pi]$ (%)	3.20	0.72	4.47	2.89
$AC1[\Delta_c]$	0.47	0.12	3.85	0.24	$AC1[\pi]$	0.83	0.13	6.59	0.86
$Skew[\Delta_c]$	-1.56	0.77	-2.03	-0.70	$Skew[\pi]$	-0.66	1.29	-0.51	1.34
$Kurt[\Delta_c]$	10.42	2.37	4.39	7.89	$Kurt[\pi]$	8.73	2.30	3.79	6.15
Panel B: 1947-2018									
$E[\Delta_c]$ (%)	1.92	0.17	11.23	1.92	$E[\pi]$ (%)	3.00	0.35	8.51	2.07
$\sigma[\Delta_c]$ (%)	1.19	0.11	11.14	1.19	$\sigma[\pi]$ (%)	2.26	0.32	7.05	2.25
$AC1[\Delta_c]$	0.48	0.12	4.01	0.24	$AC1[\pi]$	0.75	0.11	6.67	0.30
$Skew[\Delta_c]$	-0.38	0.24	-1.58	-0.28	$Skew[\pi]$	1.39	0.30	4.67	1.03
$Kurt[\Delta_c]$	2.92	0.48	6.10	3.70	$Kurt[\pi]$	4.73	1.30	3.63	5.19

Table 3: Asset Pricing Implications in Population

In this table, we report the term structure of nominal interest rates and the corresponding volatilities, first order autocorrelation, skewness, and kurtosis. All asset pricing implications in population are based on simulations of 300,000 months of data. Data statistics are based on the Fama-Bliss zero-coupon database from CRSP over the sample period 1964 until 2018.

Maturity	1y	2y	3y	4y	5y
Nominal Term structure of Interest Rates – Model					
Panel A: 1964.01-2018.12					
Mean Yield (%)	5.16	5.34	5.51	5.69	5.86
Std (%)	2.08	1.93	1.83	1.76	1.72
Nominal Term structure of Interest Rates – Data					
Panel B: 1964.01-2018.12					
Mean Yield (%)	5.16	5.37	5.56	5.73	5.84
Std (%)	3.33	3.27	3.19	3.11	3.03
Panel C: 1964.01-1981.12					
Mean Yield (%)	6.99	7.01	7.06	7.09	7.11
Std (%)	2.72	2.58	2.45	2.40	2.35
Panel D: 1982.01-2018.12					
Mean Yield (%)	4.24	4.54	4.80	5.03	5.19
Std (%)	3.18	3.23	3.20	3.15	3.09
Panel E: 2009.01-2018.12					
Mean Yield (%)	0.62	0.85	1.12	1.42	1.67
Std (%)	0.68	0.67	0.64	0.62	0.61

Table 4: Benchmark Bond Predictability Regressions

Panel A reports the restricted Cochrane-Piazzesi regressions from the projection of holding period returns on the single CP factor; Panel B reports the Fama-Bliss regression results from the projection of holding period returns on forward-spot spreads; Panel C reports the Campbell-Shiller regressions from the projection of changes in long rate spreads on yield-spot spreads; Panel D reports the Dai-Singleton regressions from the projection of adjusted changes in long rate spreads on yield-spot spreads. Data statistics are based on the Fama-Bliss zero-coupon database from CRSP over the sample period 1964 until 2018.

Model					Data				
Panel A: Cochrane-Piazzesi: regression of holding period returns on single CP factor									
$rx_{n,t+12} = b_n \left(\gamma^\top f_t \right) + \varepsilon_{n,t+12}$									
	$n = 2$	$n = 3$	$n = 4$	$n = 5$		$n = 2$	$n = 3$	$n = 4$	$n = 5$
b_n	0.42	0.82	1.20	1.56	b_n	0.45	0.85	1.25	1.46
HH,12 lags	0.01	0.02	0.02	0.03	HH,12 lags	0.08	0.16	0.22	0.27
R^2	0.19	0.19	0.20	0.20	R^2	0.20	0.22	0.25	0.23
Panel B: Fama-Bliss: regression of holding period returns on forward-spot spread									
$rx_{n,t+12} = \alpha_n + \beta_n \left(f_{n,t} - y_{1,t}^{\$} \right) + \varepsilon_{n,t+12}$									
	$n = 2$	$n = 3$	$n = 4$	$n = 5$		$n = 2$	$n = 3$	$n = 4$	$n = 5$
β_n	0.78	0.82	0.86	0.90	β_n	0.84	1.14	1.36	1.12
HH,12 lags	0.02	0.02	0.02	0.02	HH,12 lags	0.26	0.33	0.39	0.43
NW,18 lags	0.02	0.02	0.02	0.02	NW,18 lags	0.23	0.29	0.34	0.39
R^2	0.09	0.10	0.10	0.11	R^2	0.12	0.14	0.15	0.09
Panel C: Campbell-Shiller: regression of changes in long rate spreads on yield-spot spread									
$y_{n-1,t+12}^{\$} - y_{n,t}^{\$} = \alpha_n + \beta_n \frac{1}{n-1} \left(y_{n,t}^{\$} - y_{1,t}^{\$} \right) + \varepsilon_{n,t+12}$									
	$n = 2$	$n = 3$	$n = 4$	$n = 5$		$n = 2$	$n = 3$	$n = 4$	$n = 5$
β_n	-0.56	-0.60	-0.64	-0.67	β_n	-0.67	-1.08	-1.48	-1.51
HH,12 lags	0.04	0.04	0.04	0.04	HH,12 lags	0.52	0.62	0.67	0.71
NW,18 lags	0.04	0.04	0.04	0.04	NW,18 lags	0.47	0.55	0.59	0.63
R^2	0.01	0.02	0.02	0.02	R^2	0.02	0.04	0.07	0.06
Panel D: Dai-Singleton: regression of adjusted changes in long rate spreads on yield-spot spread									
$y_{n-1,t+12}^{\$} - y_{n,t}^{\$} + \frac{1}{n-1} \hat{E}_t \left[r_{n,t+12} - y_{1,t}^{\$} \right] = \alpha_n + \beta_n \frac{1}{n-1} \left(y_{n,t}^{\$} - y_{1,t}^{\$} \right) + \varepsilon_{n,t+12}$									
	$n = 2$	$n = 3$	$n = 4$	$n = 5$		$n = 2$	$n = 3$	$n = 4$	$n = 5$
β_n	0.99	0.99	1.00	1.00	β_n	1.08	1.12	1.02	0.73
HH,12 lags	0.04	0.04	0.04	0.04	HH,12 lags	0.46	0.56	0.61	0.64
NW,18 lags	0.04	0.04	0.04	0.04	NW,18 lags	0.42	0.50	0.54	0.57
R^2	0.04	0.04	0.05	0.05	R^2	0.06	0.05	0.04	0.02

Table 5: Model Extensions – Moments

In this table, we present asset pricing moments for the benchmark model with only consumption growth volatility σ_t (GDA1), with constant volatility and time-varying expected growth x_t (GDA2), and with both time-varying expected growth and consumption growth volatility (GDA3). We also present the three models with standard recursive utility without disappointment aversion (EZ1, EZ2, EZ3). Panel A describes each model. Panel B reports the calibrated values of the preference parameters; in Panel C, we present moments of real per capita consumption and inflation dynamics; in Panel D, we present asset price moments for the level and the slope of the nominal yield curve, and the first moment, the second moment, and the autocorrelation coefficient of the equity return, the risk-free rate, and the log price-dividend ratio. We report population statistics based on a simulation of 300,000 months. We use the CRSP Fama-Bliss zero-coupon database between 1964 and 2018, the BEA NIPA consumption and inflation data between 1929 and 2018, and CRSP stock and dividend price data between 1929 and 2018. Cash flow data are real and sampled at an annual frequency. Consumption and price growth rates in the model are time-averaged.

Panel A: Model	Data	GDA1	GDA2	GDA3	EZ1	EZ2	EZ3
x_t	–		✓	✓		✓	✓
σ_t	–	✓		✓	✓		✓
Panel B: Preferences							
δ	–	0.9985	0.9987	0.9957	0.9989	0.9988	0.9958
ψ	–	1.5	1.5	∞	1.5	2.0	∞
γ	–	2.0	2.0	2.0	5.0	18	9.5
ℓ	–	1.0	1.0	1.0	–	–	–
κ	–	0.950	0.990	0.971	–	–	–
Panel C: Cash flows							
$E[\Delta_c]$ (%)	1.94	1.79	1.82	1.79	1.79	1.82	1.79
$\sigma[\Delta_c]$ (%)	1.93	2.08	1.95	1.94	2.08	1.95	1.94
$AC1[\Delta_c]$	0.47	0.24	0.57	0.56	0.24	0.57	0.56
$Skew[\Delta_c]$	-1.56	-0.70	0.01	-1.54	-0.70	0.01	-1.54
$Kurt[\Delta_c]$	10.42	7.89	2.96	8.73	7.89	2.96	8.73
$E[\pi]$ (%)	3.00	3.57	3.51	3.55	3.57	3.51	3.55
$\sigma[\pi]$ (%)	3.20	2.89	2.91	2.89	2.89	2.91	2.89
$AC1[\pi]$	0.83	0.86	0.87	0.86	0.86	0.87	0.86
$Skew[\pi]$	-0.66	1.34	0.82	1.26	1.34	0.82	1.26
$Kurt[\pi]$	8.73	6.15	4.95	5.88	6.15	4.95	5.88
Panel D: Asset Pricing Moments							
$E[y_1^s]$ (%)	5.16	5.16	5.17	5.16	5.12	5.17	5.11
$E[y_5^s - y_1^s]$ (%)	0.68	0.70	0.68	0.69	0.67	0.70	0.70
$E[r]$ (%)	5.56	5.70	5.59	6.86	5.14	5.06	9.05
$\sigma[r]$ (%)	19.01	17.50	17.64	16.49	14.77	17.85	17.38
$AC1[r]$	0.02	-0.01	0.02	0.02	-0.03	0.02	0.03
$E[r_f]$ (%)	0.58	1.27	1.25	1.33	1.23	1.26	1.28
$\sigma[r_f]$ (%)	3.94	1.98	0.63	2.58	1.32	0.47	2.50
$AC1[r_f]$	0.62	0.96	0.82	0.92	0.96	0.82	0.94
$E[p - d]$ (%)	3.39	3.02	3.04	2.79	3.12	3.15	2.50
$\sigma[p - d]$ (%)	0.46	0.33	0.05	0.15	0.27	0.06	0.18
$AC1[p - d]$	0.87	0.93	0.82	0.94	0.90	0.82	0.94

Table 6: Model Extensions – Predictability

We present models when agents exhibit disappointment aversion (GDA) and when they have standard recursive utility preferences (EZ). For each set of preferences, we report predictability results when consumption growth has time-varying volatility (GDA1, EZ1), time-varying conditional mean (GDA2, EZ2), both time-varying conditional mean and volatility (GDA3, EZ3). We report results for the Cochrane-Piazzesi regressions (Panel B), the Fama-Bliss regressions (Panel C), the Campbell-Shiller regressions (Panel D), the regressions of future excess stock returns on the log price-dividend ratio (Panel E), the regressions of future consumption growth on the log price-dividend ratio (Panel F). We report population statistics based on a simulation of 300,000 months. We use the CRSP Fama-Bliss zero-coupon database between 1964 and 2018, the BEA NIPA consumption and inflation data between 1929 and 2018, and CRSP stock and dividend price data between 1929 and 2018.

	Data	GDA1	GDA2	GDA3	EZ1	EZ2	EZ3
Panel A: Preferences							
δ	–	0.9985	0.9987	0.9957	0.9989	0.9988	0.9958
ψ	–	1.5	1.5	∞	1.5	2.0	∞
γ	–	2.0	2.0	2.0	5.0	18	9.5
ℓ	–	1.0	1.0	1.0	–	–	–
κ	–	0.950	0.990	0.971	–	–	–
Panel B: Predictability of Excess Bond Returns – Cochrane-Piazzesi regressions							
$[b(2)]$	0.45	0.42	0.46	0.41	0.44	0.47	0.39
$R^2(2)$ (%)	19.89	18.84	0.00	18.91	11.08	0.001	21.97
$[b(5)]$	1.46	1.56	1.49	1.58	1.53	1.47	1.62
$R^2(5)$ (%)	23.31	20.02	0.00	22.31	11.19	0.00	27.41
Panel C: Predictability of Excess Bond Returns – Fama-Bliss regressions							
$[b(2)]$	0.84	0.78	0.00	0.71	0.53	0.00	0.76
$R^2(2)$ (%)	11.66	9.14	0.00	11.17	2.62	0.00	13.93
$[b(5)]$	1.12	0.90	0.01	0.80	0.61	0.01	0.89
$R^2(5)$ (%)	9.00	11.15	0.00	14.38	2.99	0.00	19.60
Panel D: Predictability of Excess Bond Returns – Campbell-Shiller regressions							
$[b(2)]$	-0.67	-0.56	1.00	-0.42	-0.06	1.00	-0.51
$R^2(2)$ (%)	2.06	1.28	2.30	1.08	0.00	2.30	1.81
$[b(5)]$	-0.151	-0.67	0.98	-0.48	-0.11	0.98	-0.65
$R^2(5)$ (%)	6.13	1.92	2.65	1.74	0.00	2.66	3.51
Panel E: Predictability of Excess Stock Returns by log(P/D) ratio							
$[b(1)]$	-0.06	-0.16	0.01	-0.28	-0.13	0.01	-0.28
$R^2(1)$ (%)	9.37	9.29	0.00	6.44	5.88	0.00	8.58
$[b(5)]$	-0.07	-0.14	-0.02	-0.25	-0.12	-0.02	-0.25
$R^2(5)$ (%)	20.74	36.90	0.02	24.15	24.90	0.01	31.55
Panel F: Predictability of Consumption Growth by log(P/D) ratio							
$[b(1)]$	0.01	0.00	0.20	0.05	0.01	0.18	0.04
$R^2(1)$ (%)	3.21	0.38	28.71	15.36	0.35	28.71	14.66
$[b(5)]$	-0.004	0.00	0.11	0.03	0.001	0.10	0.02
$R^2(5)$ (%)	4.34	0.11	16.87	9.28	0.09	16.87	8.88

Figure 1: Model Solutions

In Figure 1a, we plot the welfare valuation ratio $V_t/C_t = G^V(\sigma_t^2)$ as a function of consumption volatility σ_t^2 for our benchmark scenario with 501 grid points. In Figure 1b, we plot the welfare valuation ratio $V_t/C_t = G^V(\sigma_t^2)$ as a function of consumption volatility σ_t^2 for different grids, ranging from 24 to 750 points. In Figure 1c, we report the probability of disappointment $\xi(\sigma_t^2)$ as a function of consumption volatility σ_t^2 . In Figure 1d, we plot the welfare valuation ratio $V_t/C_t = G^V(\sigma_t^2)$ as a function of consumption volatility, σ_t^2 , for an investor with Epstein-Zin recursive utility, i.e., without disappointment aversion. For this case, we report both the analytical solution (solid line) and the numerical solution (dotted line) for our benchmark scenario with 501 grid points. The consumption growth parameters are identical to those reported for the model GDA1 in Table 1. The preference parameters for this example are $\delta = 0.9989$, $\psi = 1$, and $\gamma = 4$.

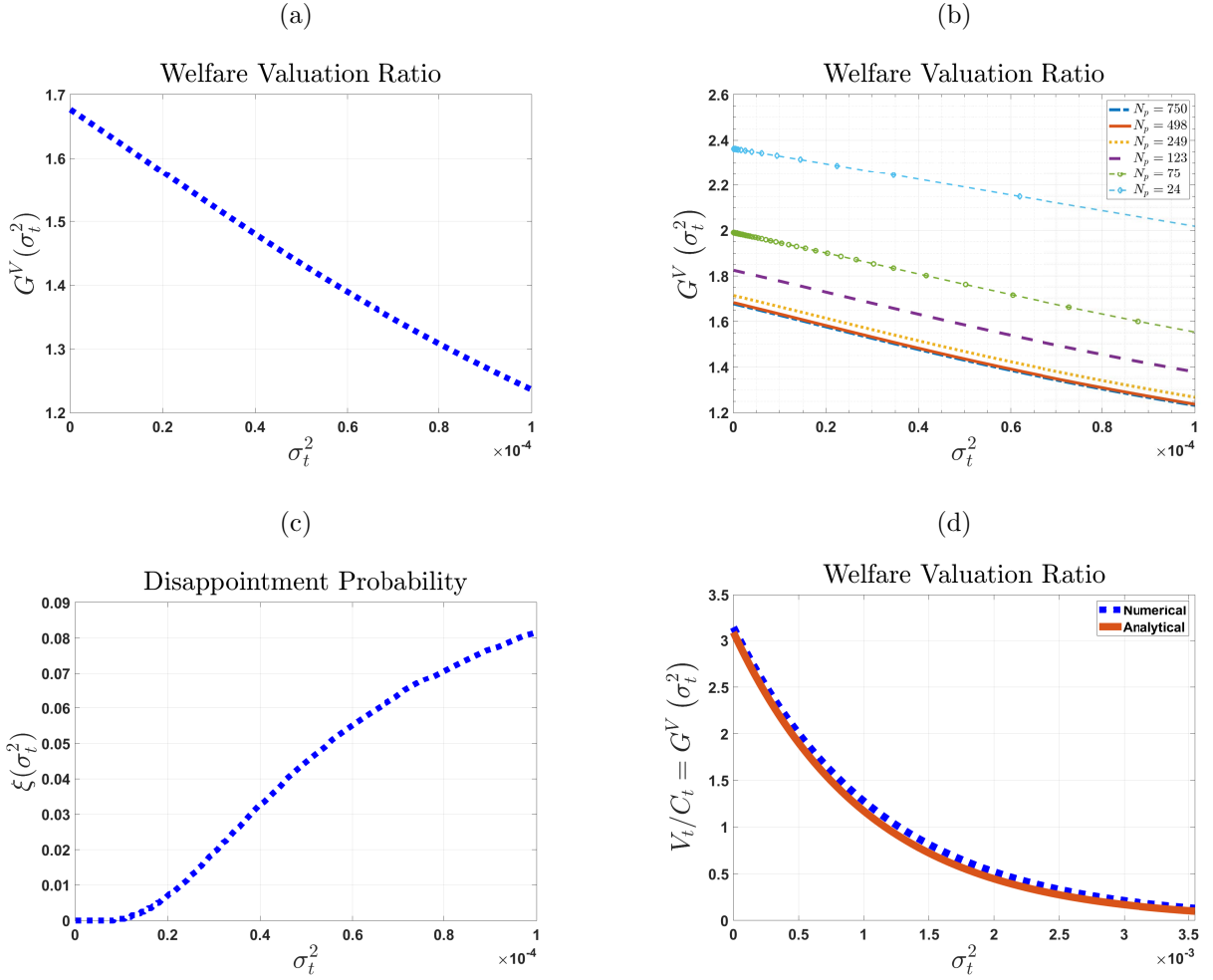


Figure 2: Asset Pricing Solutions

In this figure, we plot asset pricing solutions for our benchmark scenario with 501 grid points. In Figure 2a, we plot the real yields $y_{n,t}$ as a function of consumption volatility for maturities $n = 1$ year to $n = 5$ years. In Figures 2b and 2c, we plot the sensitivities of nominal bond yields $y_{n,t}^s$ to expected inflation ($-B_{z,n}^s/n$) and inflation volatility ($-B_{v,n}^s/n$), respectively. In Figure 2d, we plot nominal bond yields, $y_{n,t}^s$, as a function of consumption volatility for maturities $n = 1$ year to $n = 5$ years when expected inflation and inflation uncertainty are fixed at their long-run values.

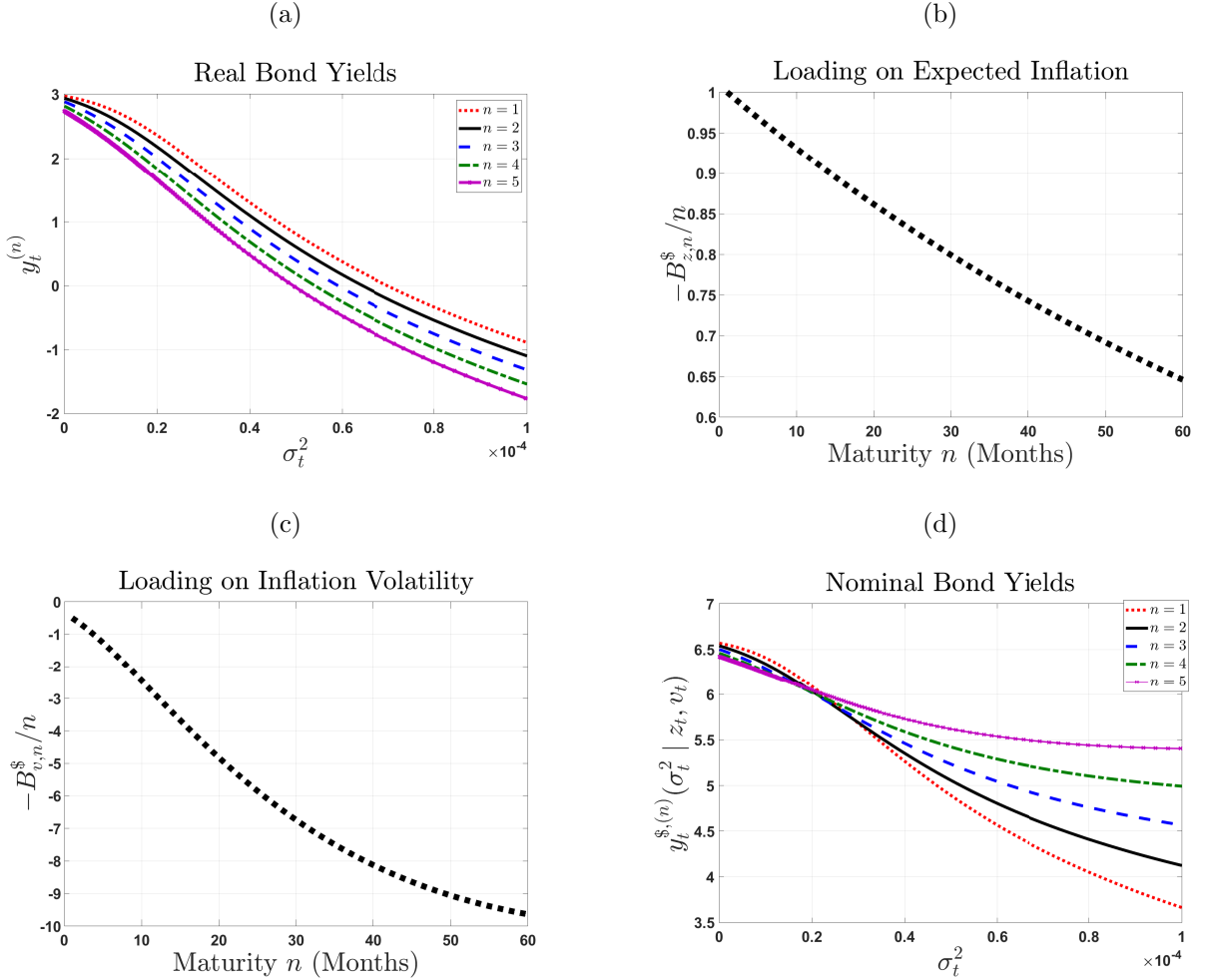
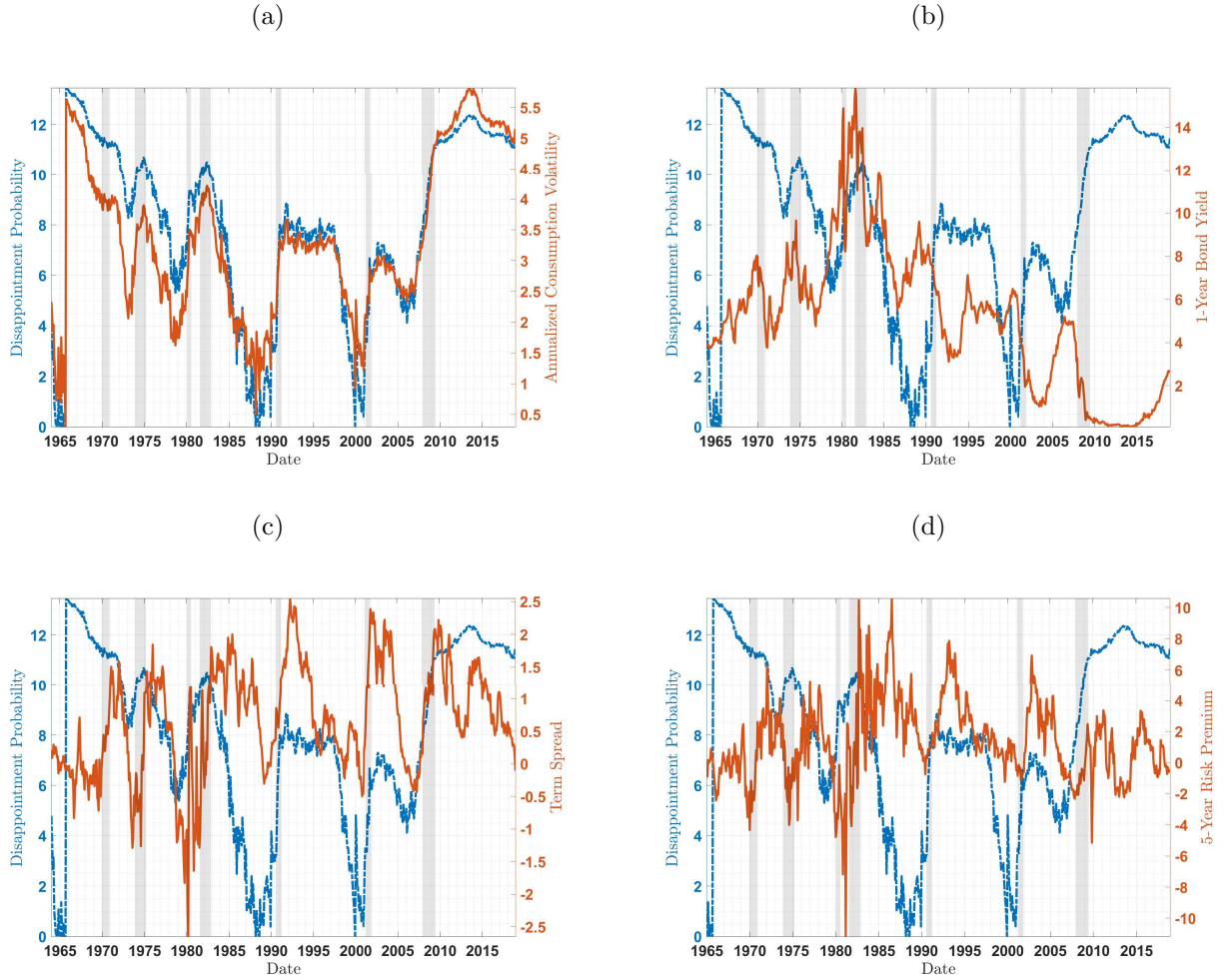


Figure 3: Disappointment Probability and the Term Structure of Interest Rates

In this figure, we plot the filtered disappointment probability together with annualized consumption volatility in Figure 3a, with the one-year nominal bond yield ($y_{1,y}^{\$}$) in Figure 3b, with the nominal term spread ($y_{5,y}^{\$} - y_{1,y}^{\$}$) in Figure 3c, and with the five-year bond risk premium in Figure 3d. Consumption volatility is inferred from observed monthly real per capita consumption growth data available from the FRED database, and using calibrated parameters of our benchmark consumption dynamics. Disappointment probability is implied by the filtered series of consumption volatility, using the calibrated preference parameters from our benchmark model specification. The risk premium on a 5-year bond is estimated based on the Cochrane and Piazzesi (2005) factor in the data. Grey bars indicate NBER recession dates. The sample period is from January 1964 to December 2018.



A Solutions to Welfare Valuation Ratios

The welfare valuation ratios are defined as:

$$\frac{V_t}{C_t} = G^V(\mathbf{X}_t) \quad \text{and} \quad \frac{\mathcal{R}_t(V_{t+1})}{C_t} = G^{\mathcal{R}}(\mathbf{X}_t), \quad (\text{A.1})$$

where \mathbf{X}_t characterizes the N -dimensional state vector that governs the real economy. Define the function $Z^{\mathcal{R}}(\cdot; \cdot)$ as:

$$Z^{\mathcal{R}}(\cdot; \cdot) = F(G^{\mathcal{R}}(\mathcal{S}(\cdot; \cdot))) \exp(\mathcal{O}(\cdot; \cdot)), \quad (\text{A.2})$$

where $\mathcal{O}(\cdot; \cdot)$ and $\mathcal{S}(\cdot; \cdot)$ characterize two generic functions describing the observation and state equations in a state-space system, which we have specified as:

$$\begin{aligned} \Delta c_{t+1} &= \mathcal{O}(\mathcal{E}_{t+1}; \mathbf{X}_t) \\ \mathbf{X}_{t+1} &= \mathcal{S}(\mathcal{E}_{t+1}; \mathbf{X}_t), \end{aligned} \quad (\text{A.3})$$

with \mathcal{E}_{t+1} being a K -dimensional vector of independent and identically distributed shocks with density function $h(\mathcal{E})$ and support $\mathbb{E} \subseteq \mathbb{R}^K$. It follows from the recursion in Equation (2) and the certainty equivalent in Equation (5) that:

$$\begin{aligned} G^{\mathcal{R}}(\mathbf{X}_t) &= \left(\frac{E_t \left[(1 + \ell I(Z^{\mathcal{R}}(\mathcal{E}_{t+1}; \mathbf{X}_t) < \kappa G^{\mathcal{R}}(\mathbf{X}_t))) (Z^{\mathcal{R}}(\mathcal{E}_{t+1}; \mathbf{X}_t))^{1-\gamma} \right]}{1 + \ell \kappa^{1-\gamma} E_t [I(Z^{\mathcal{R}}(\mathcal{E}_{t+1}; \mathbf{X}_t) < \kappa G^{\mathcal{R}}(\mathbf{X}_t))]} \right)^{\frac{1}{1-\gamma}} \\ &= \left(\frac{\int_{\mathbb{E}} (1 + \ell I(Z^{\mathcal{R}}(\mathcal{E}; \mathbf{X}_t) < \kappa G^{\mathcal{R}}(\mathbf{X}_t))) (Z^{\mathcal{R}}(\mathcal{E}; \mathbf{X}_t))^{1-\gamma} h(\mathcal{E}) d\mathcal{E}}{1 + \ell \kappa^{1-\gamma} \int_{\mathbb{E}} I(Z^{\mathcal{R}}(\mathcal{E}; \mathbf{X}_t) < \kappa G^{\mathcal{R}}(\mathbf{X}_t)) h(\mathcal{E}) d\mathcal{E}} \right)^{\frac{1}{1-\gamma}}, \end{aligned} \quad (\text{A.4})$$

where $\int_{\mathbb{E}}$ defines the integral over the domain \mathbb{E} . We solve Equation (A.4) recursively using numerical integration. We initiate the recursion by conjecturing a solution $G_0^{\mathcal{R}}(\mathbf{X}_t)$. $G_1^{\mathcal{R}}(\mathbf{X}_t)$ is then obtained on a grid of values for \mathbf{X}_t , as:

$$G_1^{\mathcal{R}}(\mathbf{X}_t) = \left(\frac{\int_{\mathbb{E}} (1 + \ell I(Z_0^{\mathcal{R}}(\mathcal{E}; \mathbf{X}_t) < \kappa G_0^{\mathcal{R}}(\mathbf{X}_t))) (Z_0^{\mathcal{R}}(\mathcal{E}; \mathbf{X}_t))^{1-\gamma} h(\mathcal{E}) d\mathcal{E}}{1 + \ell \kappa^{1-\gamma} \int_{\mathbb{E}} I(Z_0^{\mathcal{R}}(\mathcal{E}; \mathbf{X}_t) < \kappa G_0^{\mathcal{R}}(\mathbf{X}_t)) h(\mathcal{E}) d\mathcal{E}} \right)^{\frac{1}{1-\gamma}}, \quad (\text{A.5})$$

where $Z_0^{\mathcal{R}}(\mathcal{E}; \mathbf{X}_t) = F(G_0^{\mathcal{R}}(\mathcal{S}(\mathcal{E}; \mathbf{X}_t))) \exp(\mathcal{O}(\mathcal{E}; \mathbf{X}_t))$. More generally, for any k , given a value for $G_k^{\mathcal{R}}(\mathbf{X}_t)$, we obtain the value of $G_{k+1}^{\mathcal{R}}(\mathbf{X}_t)$ on a grid of values for \mathbf{X}_t , as:

$$G_{k+1}^{\mathcal{R}}(\mathbf{X}_t) = \left(\frac{\int_{\mathbb{E}} (1 + \ell I(Z_k^{\mathcal{R}}(\mathcal{E}; \mathbf{X}_t) < \kappa G_k^{\mathcal{R}}(\mathbf{X}_t))) (Z_k^{\mathcal{R}}(\mathcal{E}; \mathbf{X}_t))^{1-\gamma} h(\mathcal{E}) d\mathcal{E}}{1 + \ell \kappa^{1-\gamma} \int_{\mathbb{E}} I(Z_k^{\mathcal{R}}(\mathcal{E}; \mathbf{X}_t) < \kappa G_k^{\mathcal{R}}(\mathbf{X}_t)) h(\mathcal{E}) d\mathcal{E}} \right)^{\frac{1}{1-\gamma}}, \quad (\text{A.6})$$

where $Z_k^{\mathcal{R}}(\mathcal{E}; \mathbf{X}_t) = F(G_k^{\mathcal{R}}(\mathcal{S}(\mathcal{E}; \mathbf{X}_t))) \exp(\mathcal{O}(\mathcal{E}; \mathbf{X}_t))$. The iterations are repeated until convergence to the fixed point, which is the solution $G^{\mathcal{R}}(\mathbf{X}_t)$ to Equation (A.4). This

solution is unique, as is discussed in Backus et al. (2004) and also shown in Marinacci and Montrucchio (2010). Given the solutions of $G^{\mathcal{R}}$, we derive the solution of $G^V = F(G^{\mathcal{R}})$. It is then straightforward to compute the disappointment probability ξ_t as:

$$\begin{aligned}\xi_t \equiv \xi(\mathbf{X}_t) &= E_t [I(Z^{\mathcal{R}}(\mathcal{E}_{t+1}; \mathbf{X}_t) < \kappa G^{\mathcal{R}}(\mathbf{X}_t))] \\ &= \int_{\mathbb{E}} I(Z^{\mathcal{R}}(\mathcal{E}; \mathbf{X}_t) < \kappa G^{\mathcal{R}}(\mathbf{X}_t)) h(\mathcal{E}) d\mathcal{E}.\end{aligned}\tag{A.7}$$

It follows from Equation (A.1) that the real stochastic discount factor is given by:

$$\begin{aligned}M_{t,t+1} &= \delta \exp(-\gamma \Delta c_{t+1}) \left(\frac{G^V(\mathbf{X}_{t+1})}{G^{\mathcal{R}}(\mathbf{X}_t)} \right)^{\frac{1}{\psi} - \gamma} \\ &\quad \times \left(\frac{1 + \ell I(G^V(\mathbf{X}_{t+1})(C_{t+1}/C_t) < \kappa G^{\mathcal{R}}(\mathbf{X}_t))}{1 + \ell \kappa^{1-\gamma} \xi(\mathbf{X}_t)} \right),\end{aligned}\tag{A.8}$$

which is derived given the solutions to the welfare valuation ratios V_t/C_t and $\mathcal{R}_t(V_{t+1})/C_t$ based on Equation (A.4), and the disappointment probability in Equation (A.7).

B Solutions to Real and Nominal Bond Prices

The term structure of real interest rates is solved recursively, given that the price $P_{n,t} \equiv P_n(\mathbf{X}_t)$ of the n -period zero-coupon real bond satisfies the recursion:

$$P_n(\mathbf{X}_t) = E_t [M_{t,t+1} P_{n-1}(\mathbf{X}_{t+1})],\tag{B.1}$$

with the initial condition $P_{0,t} = 1$. The real bond price is computed recursively using numerical integration as follows:

$$\begin{aligned}P_n(\mathbf{X}_t) &= \delta \left(\frac{1}{G^{\mathcal{R}}(\mathbf{X}_t)} \right)^{\frac{1}{\psi} - \gamma} \left(\frac{1}{1 + \ell \kappa^{1-\gamma} \xi(\mathbf{X}_t)} \right) \\ &\quad \times \int_{\mathbb{E}} \left\{ \exp(-\gamma \mathcal{O}(\mathcal{E}; \mathbf{X}_t)) (G^V(\mathcal{S}(\mathcal{E}; \mathbf{X}_t)))^{\frac{1}{\psi} - \gamma} \right. \\ &\quad \left. \times (1 + \ell I(Z^{\mathcal{R}}(\mathcal{E}; \mathbf{X}_t) < \kappa G^{\mathcal{R}}(\mathbf{X}_t))) P_{n-1}(\mathcal{S}(\mathcal{E}; \mathbf{X}_t)) \right\} h(\mathcal{E}) d\mathcal{E}.\end{aligned}\tag{B.2}$$

To derive the solution for nominal bond prices, assume that the dynamics of the inflation rate process are governed by an L -dimensional real-valued vector process \mathbf{Y}_t such that the joint moment generating function, conditional on the real vector of shocks \mathcal{E}_{t+1} , is given by:

$$E_t [\exp(a\pi_{t+1} + b^\top \mathbf{Y}_{t+1}) | \mathcal{E}_{t+1}] = \exp(A(a, b, \mathbf{X}_t, \mathcal{E}_{t+1}) + \mathbf{Y}_t^\top B(a, b)).\tag{B.3}$$

Given the assumption for the inflation dynamics, we conjecture and verify that:

$$P_{n,t}^{\$} = P_n^{\$}(\mathbf{X}_t) \exp(\mathbf{Y}_t^\top B_n^{\$}),\tag{B.4}$$

where the coefficients $B_n^\$$ satisfy the recursion $B_n^\$ = B(-1, B_{n-1}^\$)$, with the initial vector-valued condition $B_0^\$ = \mathbf{0}$. We use the law of iterated expectations to ensure that the numerical integration applies only to the vector of real shocks \mathcal{E}_t . This allows us to derive the recursion for the sequence $\{P_n^\$(\mathbf{X}_t)\}$ as follows:

$$P_n^\$(\mathbf{X}_t) = E_t \left[M_{t,t+1} P_{n-1}^\$(\mathbf{X}_{t+1}) \exp \left(A(-1, B_{n-1}^\$, \mathbf{X}_t, \mathcal{E}_{t+1}) \right) \right], \quad (\text{B.5})$$

with the initial condition $P_0^\$(\mathbf{X}_t) = 1$. The recursion (B.5) has no closed-form solution and is solved by numerical integration over a grid of values for \mathbf{X}_t . It follows that:

$$\begin{aligned} P_n^\$(\mathbf{X}_t) &= \delta \left(\frac{1}{G^\mathcal{R}(\mathbf{X}_t)} \right)^{\frac{1}{\psi} - \gamma} \left(\frac{1}{1 + \ell \kappa^{1-\gamma} \xi(\mathbf{X}_t)} \right) \\ &\times \int_{\mathbb{E}} \left\{ \exp \left(-\gamma \mathcal{O}(\mathcal{E}; \mathbf{X}_t) + A(-1, B_{n-1}^\$, \mathbf{X}_t, \mathcal{E}_{t+1}) \right) (G^V(\mathcal{S}(\mathcal{E}; \mathbf{X}_t)))^{\frac{1}{\psi} - \gamma} \right. \\ &\quad \times \left. (1 + \ell I(Z^\mathcal{R}(\mathcal{E}; \mathbf{X}_t) < \kappa G^\mathcal{R}(\mathbf{X}_t))) P_{n-1}^\$(\mathcal{S}(\mathcal{E}; \mathbf{X}_t)) \right\} h(\mathcal{E}) d\mathcal{E}. \end{aligned} \quad (\text{B.6})$$

C Welfare Valuation Ratios with Recursive Utility

We derive solutions to the welfare valuation ratios when the representative investor has Epstein and Zin (1989) preferences, without disappointment version ($\ell = 0$), and the Kreps and Porteus (1978) certainty equivalent. Define the log welfare valuation ratios $z_{V,t} = \ln(C_t / V_t)$ and $z_{\mathcal{R},t} = \ln(C_t / \mathcal{R}_t(V_{t+1}))$, which are given by the two recursions:

$$\begin{aligned} z_{V,t} &= -\frac{1}{1 - \frac{1}{\psi}} \ln \left((1 - \delta) + \delta \exp \left(-\left(1 - \frac{1}{\psi}\right) z_{\mathcal{R},t} \right) \right) \quad \text{if } \psi \neq 1 \\ &= \delta z_{\mathcal{R},t} \quad \text{if } \psi = 1, \end{aligned} \quad (\text{C.1})$$

and

$$\begin{aligned} z_{\mathcal{R},t} &= -\frac{1}{1 - \gamma} \ln \left(E_t [\exp((1 - \gamma)(\Delta c_{t+1} - z_{V,t+1}))] \right) \quad \text{if } \gamma \neq 1, \\ &= E_t [z_{V,t+1} - \Delta c_{t+1}] \quad \text{if } \gamma = 1. \end{aligned} \quad (\text{C.2})$$

Solving for these ratios is standard in the literature and necessitates the use of the affine property of the dynamics of consumption growth, in conjunction with the log-linear approximation of the first recursion in Equation (C.1) around the average log welfare valuation ratio $\bar{z}_{\mathcal{R}} = E[z_{\mathcal{R},t}]$,

$$z_{V,t} = q_0 + q_1 z_{\mathcal{R},t}, \quad (\text{C.3})$$

where

$$q_1 = \frac{\delta \exp \left(- \left(1 - \frac{1}{\psi} \right) \bar{z}_{\mathcal{R}} \right)}{(1 - \delta) + \delta \exp \left(- \left(1 - \frac{1}{\psi} \right) \bar{z}_{\mathcal{R}} \right)} \text{ and } q_0 = \frac{1}{1 - \frac{1}{\psi}} \left[q_1 \ln \frac{(1 - \delta) q_1}{\delta (1 - q_1)} - \ln \frac{1 - \delta}{1 - q_1} \right]. \quad (\text{C.4})$$

These coefficients are equivalent to the coefficients of the log-linear approximation of Campbell and Shiller (1988a) of the unobserved return on the claim over future consumption stream, around the average consumption-wealth ratio.

Given the consumption growth dynamics defined in Equation (17), and the conjecture

$$z_{V,t} = \beta_{V0} + \beta_{V\sigma} \sigma_t^2 \text{ and } z_{\mathcal{R},t} = \beta_{\mathcal{R}0} + \beta_{\mathcal{R}\sigma} \sigma_t^2, \quad (\text{C.5})$$

we use the method of undetermined coefficients and the property that

$$E \left[\exp (a\epsilon^2 + b\epsilon) \right] = \exp \left(-\frac{1}{2} \ln (1 - 2a) + \frac{b^2}{2(1 - 2a)} \right) \quad (\text{C.6})$$

for any real numbers a and b and any standard normal random variable ϵ , to show that:

$$\begin{aligned} \beta_{\mathcal{R}0} &= \beta_{V0} - \mu_c + \beta_{V\sigma} ((1 - \phi_{\sigma}) \mu_{\sigma} - \nu_{\sigma}) + \frac{\ln (1 + 2(1 - \gamma) \nu_{\sigma} \beta_{V\sigma})}{2(1 - \gamma)} \\ \beta_{\mathcal{R}\sigma} &= \phi_{\sigma} \beta_{V\sigma} - \frac{(1 - \gamma) (1 + 2\nu_{\sigma} \beta_{V\sigma} \beta_{\sigma})^2}{2(1 + 2(1 - \gamma) \nu_{\sigma} \beta_{V\sigma})}. \end{aligned} \quad (\text{C.7})$$

The parameter $\bar{z}_{\mathcal{R}}$ is endogenous to the recursive utility model, and can be found as the solution to the non-linear fixed-point equation $\bar{z}_{\mathcal{R}} = \beta_{\mathcal{R}0} + \beta_{\mathcal{R}\sigma} \mu_{\sigma}$, since $\beta_{\mathcal{R}0}$ and $\beta_{\mathcal{R}\sigma}$ depend on q_0 and q_1 , which in turn depend on $\bar{z}_{\mathcal{R}}$. The loglinear approximation $z_{V,t} = q_0 + q_1 z_{\mathcal{R},t}$ of the lifetime utility recursion implies that $\beta_{V0} = q_0 + q_1 \beta_{\mathcal{R}0}$ and $\beta_{V\sigma} = q_1 \beta_{\mathcal{R}\sigma}$, implying from Equation (C.7) that:

$$\begin{aligned} \beta_{V0} &= \frac{q_0}{1 - q_1} + \frac{q_1}{1 - q_1} \left[-\mu_c + \beta_{V\sigma} ((1 - \phi_{\sigma}) \mu_{\sigma} - \nu_{\sigma}) + \frac{\ln (1 + 2(1 - \gamma) \nu_{\sigma} \beta_{V\sigma})}{2(1 - \gamma)} \right] \\ \beta_{\mathcal{R}0} &= \frac{\beta_{V0} - q_0}{q_1} \text{ and } \beta_{\mathcal{R}\sigma} = \frac{\beta_{V\sigma}}{q_1}, \end{aligned} \quad (\text{C.8})$$

where $\beta_{V\sigma}$ is solution to the quadratic equation

$$\beta_{V\sigma}^2 - S\beta_{V\sigma} + P = 0, \quad (\text{C.9})$$

with

$$\begin{aligned} S &= -\frac{(1 - q_1 \phi_{\sigma}) + 2(1 - \gamma) q_1 \nu_{\sigma} \beta_{\sigma}}{2(1 - \gamma) \nu_{\sigma} (1 - q_1 (\phi_{\sigma} - \nu_{\sigma} \beta_{\sigma}^2))} \\ P &= \frac{q_1}{4\nu_{\sigma} (1 - q_1 (\phi_{\sigma} - \nu_{\sigma} \beta_{\sigma}^2))}. \end{aligned} \quad (\text{C.10})$$

Given the calibrated volatility parameters implying $\beta_\sigma > 0$, the quantities S and P are real and the quantity $S^2 - 4P$ is nonnegative as long as γ is smaller than γ^{max} , where γ^{max} is the largest value beyond which the model does not allow for a converging solution. In this case, the two solutions $\beta_{V\sigma}^-$ and $\beta_{V\sigma}^+$ to this equation, with $\beta_{V\sigma}^- \leq \beta_{V\sigma}^+$, are given by:

$$\beta_{V\sigma}^- = \frac{S - \sqrt{S^2 - 4P}}{2} \quad \text{and} \quad \beta_{V\sigma}^+ = \frac{S + \sqrt{S^2 - 4P}}{2}. \quad (\text{C.11})$$

We follow Bollerslev et al. (2012) and choose $\beta_{V\sigma} = \beta_{V\sigma}^-$, such that $\lim_{\alpha_\sigma \rightarrow 0} \alpha_\sigma \beta_{V\sigma}^+ = 0$.

D Model Extensions

For the analysis of equity prices, we specify a process for the dividend growth Δd_{t+1} that embeds a rich class of affine dynamics as specified in Eraker (2008), among others. We solve for the price-dividend ratio numerically using the *series method* as in Wachter (2005). The price of a claim to the aggregate dividend may be written as an infinite sum of n -period zero-coupon equity strips:

$$P_t^d = \sum_{n=1}^{\infty} E_t [M_{t,t+n} D_{t+n}] \quad \Leftrightarrow \quad \frac{P_t^d}{D_t} = \sum_{n=1}^{\infty} \frac{P_{n,t}^d}{D_t}, \quad (\text{D.1})$$

where

$$\frac{P_{n,t}^d}{D_t} = E_t \left[M_{t,t+n} \frac{D_{t+n}}{D_t} \right], \quad \text{and} \quad M_{t,t+n} = \prod_{j=1}^n M_{t+j-1,t+j}. \quad (\text{D.2})$$

To derive the solution to equity prices, we assume that the dividend dynamics are governed by an N -dimensional real-valued vector process \mathbf{Z}_t such that the joint moment generating function, conditional on the real vector of shocks \mathcal{E}_{t+1} , is given by:

$$E_t \left[\exp \left(a \Delta d_{t+1} + b^\top \mathbf{Z}_{t+1} \right) \mid \mathcal{E}_{t+1} \right] = \exp \left(A^d(a, b, \mathbf{X}_t, \mathcal{E}_{t+1}) + \mathbf{Z}_t^\top H^d(a, b) \right), \quad (\text{D.3})$$

which we use to conjecture that:

$$\frac{P_{n,t}^d}{D_t} = G_n^d(\mathbf{X}_t) \exp \left(\mathbf{Z}_t^\top B_n^d \right), \quad (\text{D.4})$$

where the coefficients B_n^d satisfy the recursion $B_n^d = H^d(1, B_{n-1}^d)$, with the initial vector-valued condition $B_0^d = \mathbf{0}$. We use the law of iterated expectations to ensure that the numerical integration applies only to the vector of real shocks \mathcal{E}_t , which allows us to show that $G_n^d(\mathbf{X}_t)$ satisfies the recursion

$$G_n^d(\mathbf{X}_t) = E_t \left[M_{t,t+1} G_{n-1}^d(\mathbf{X}_{t+1}) \exp \left(A^d(1, B_{n-1}^d, \mathbf{X}_t, \mathcal{E}_{t+1}) \right) \right], \quad (\text{D.5})$$

with initial condition $G_0^d(\mathbf{X}_t) = 1$. The recursion in Equation (D.5) has no closed-form solution and is solved by numerical integration over a grid of values for \mathbf{X}_t . It follows that:

$$G_n^d(\mathbf{X}_t) = \delta \left(\frac{1}{G^{\mathcal{R}}(\mathbf{X}_t)} \right)^{\frac{1}{\psi} - \gamma} \left(\frac{1}{1 + \ell \kappa^{1-\gamma} \xi(\mathbf{X}_t)} \right) \times \int_{\mathbb{E}} \left\{ \exp(-\gamma \mathcal{O}(\mathcal{E}; \mathbf{X}_t) + A^d(1, B_{n-1}^d, \mathbf{X}_t, \mathcal{E}_{t+1})) (G^V(\mathcal{S}(\mathcal{E}; \mathbf{X}_t)))^{\frac{1}{\psi} - \gamma} \right. \\ \left. \times (1 + \ell I(Z^{\mathcal{R}}(\mathcal{E}; \mathbf{X}_t) < \kappa G^{\mathcal{R}}(\mathbf{X}_t))) G_{n-1}^d(\mathcal{S}(\mathcal{E}; \mathbf{X}_t)) \right\} h(\mathcal{E}) d\mathcal{E}. \quad (\text{D.6})$$

To solve for equity market moments, we introduce an explicit process for the aggregate dividend growth rate. As in Bansal et al. (2009), we assume that consumption and dividends are cointegrated with cointegration parameter ϕ_d :

$$d_t - \phi_d c_t = \phi_0 + (\mu_d - \phi_d \mu_c) t + \zeta_t, \quad (\text{D.7})$$

where μ_d captures the unconditional mean dividend growth rate, and where ζ_t is an AR(1) process with persistence ϕ_ζ and shock sensitivity ν_ζ :

$$\zeta_{t+1} = \phi_\zeta \zeta_t + \nu_\zeta \sigma_t \tilde{\eta}_{t+1}, \quad (\text{D.8})$$

and where the i.i.d. standard normal shocks $\tilde{\eta}_{t+1}$ have a correlation $\rho_{\eta\varepsilon}$ with the shocks to realized consumption growth ε_{t+1} . From Equations (D.7) and (D.8), the dividend growth process may be expressed as follows

$$\Delta d_{t+1} = \mu_d - (1 - \phi_\zeta) \zeta_t + \phi_d (\Delta c_{t+1} - \mu_c) + \nu_\zeta \sigma_t \tilde{\eta}_{t+1}. \quad (\text{D.9})$$

reflecting that dividends are levered claims to aggregate consumption. The dynamics of the dividend growth Δd_{t+1} depend on the state variable $\mathbf{Z}_{t+1} = \zeta_{t+1}$, i.e., the cointegrated residual. Equation (D.9) nests the case where consumption and dividends are not cointegrated, i.e., $\phi_\zeta = 1$, as is common in the long run risk literature.

Together with Equation (17), we note that these dynamics can be mapped into the general framework defined in Equation (D.3) as follows:

$$A^d(a, b, \sigma_t^2, \varepsilon_{t+1}) = a\mu_d + \frac{1}{2} (a+b)^2 \nu_\zeta^2 (1 - \rho_{\eta\varepsilon}^2) \sigma_t^2 + (a\phi_d + (a+b) \nu_\zeta \rho_{\eta\varepsilon}) \sigma_t \varepsilon_{t+1} \quad (\text{D.10}) \\ H^d(a, b) = -a + \phi_\zeta (a+b).$$

With this specification, we show that

$$\frac{P_{n,t}^d}{D_t} = G_n^d(\sigma_t^2) \exp(B_{\zeta,n}^d \zeta_t), \quad (\text{D.11})$$

where $B_{\zeta,n}^d = -(1 - \phi_\zeta^n)$, and the sequence $\{G_n^d(\sigma_t^2)\}$ satisfies the recursion

$$G_n^d(\sigma_t^2) = \exp\left((\mu_d - \phi_d \mu_c) + \frac{1}{2} \phi_\zeta^{2n-2} \nu_\zeta^2 (1 - \rho_{\eta\varepsilon}^2) \sigma_t^2\right) \times E_t \left[M_{t,t+1} \exp(\phi_d \Delta c_{t+1}) G_{n-1}^d(\sigma_{t+1}^2) \exp(\phi_\zeta^{n-1} \rho_{\eta\varepsilon} \nu_\zeta \sigma_t \varepsilon_{t+1}) \right], \quad (\text{D.12})$$

with the initial condition $G_0^d(\sigma_t^2) = 1$. The recursion in Equation (D.12) has no closed-form solution and is solved on a grid of values for σ_t^2 . Given the price-dividend ratios of equity strips computed by numerical integration, the total equity price dividend-ratio is computed as in Equation (D.1) by truncating the infinite sum at a large number ($n^{\max} = 3000$ in our case), and finally the equity log return obtains as:

$$r_{t+1} = -\ln\left(\frac{P_t^d}{D_t}\right) + \ln\left(\frac{P_{t+1}^d}{D_{t+1}} + 1\right) + \Delta d_{t+1}. \quad (\text{D.13})$$

When we calibrate the models GDA1 and EZ1, we set $\mu_d = 0.0015$, $\phi_d = 2.5972$, $\phi_\zeta = 0.95$, $\nu_\zeta = 5.8008$, $\rho_{\eta\varepsilon} = 0$; when we calibrate the models GDA2 and EZ2, we set $\mu_d = 0.0015$, $\phi_d = 2.5972$, $\phi_\zeta = 1$, $\nu_\zeta = 9.4129$, $\rho_{\eta\varepsilon} = 0$; when we calibrate the models GDA3 and EZ3, we set $\mu_d = 0.0015$, $\phi_d = 2.5972$, $\phi_\zeta = 1$, $\nu_\zeta = 7.5340$, $\rho_{\eta\varepsilon} = 0.2250$.

Table A.1: Subsample Cash-flows – Annual Data

In this table, we present moments of real per capita consumption and inflation dynamics from the data and the model. The data are real, sampled at an annual frequency, and cover the period 1929 to 2018. Standard errors are Newey-West with one lag. For the model, we report population statistics based on a simulation of 300,000 months. Consumption and price growth rates in the model are time-averaged. Data for consumption and price growth are from the Bureau of Economic Analysis National Income and Product Accounts Tables.

Consumption				Inflation			
Moment	Estimate	SE	T-Stat	Moment	Estimate	SE	T-Stat
Panel A: 1947-1981							
$E[\Delta_c]$ (%)	2.19	0.23	9.36	$E[\pi]$ (%)	3.71	0.64	5.82
$\sigma[\Delta_c]$ (%)	1.19	0.12	10.04	$\sigma[\pi]$ (%)	2.91	0.35	8.29
$AC1[\Delta_c]$	0.30	0.22	1.37	$AC1[\pi]$	0.70	0.12	5.91
$Skew[\Delta_c]$	-0.30	0.25	-1.22	$Skew[\pi]$	0.75	0.35	2.16
$Kurt[\Delta_c]$	2.36	0.45	5.25	$Kurt[\pi]$	2.48	0.71	3.48
Panel B: 1982-2018							
$E[\Delta_c]$ (%)	1.65	0.24	6.89	$E[\pi]$ (%)	2.23	0.22	10.27
$\sigma[\Delta_c]$ (%)	1.11	0.17	6.63	$\sigma[\pi]$ (%)	1.00	0.14	7.35
$AC1[\Delta_c]$	0.66	0.13	5.05	$AC1[\pi]$	0.68	0.19	3.55
$Skew[\Delta_c]$	-0.70	0.33	-2.13	$Skew[\pi]$	0.00	0.31	0.01
$Kurt[\Delta_c]$	3.46	0.79	4.40	$Kurt[\pi]$	3.03	0.63	4.78
Panel C: 2009-2018							
$E[\Delta_c]$ (%)	1.23	0.39	3.13	$E[\pi]$ (%)	1.55	0.25	6.17
$\sigma[\Delta_c]$ (%)	0.76	0.34	2.24	$\sigma[\pi]$ (%)	0.62	0.14	4.33
$AC1[\Delta_c]$	0.88	0.45	1.96	$AC1[\pi]$	0.29	0.81	0.35
$Skew[\Delta_c]$	0.07	2.73	0.03	$Skew[\pi]$	-0.68	0.72	-0.95
$Kurt[\Delta_c]$	1.65	8.47	0.20	$Kurt[\pi]$	3.10	2.37	1.31

Table A.2: Asset Pricing Implications in Population for Post-War Sample

In this table, we report the term structure of nominal interest rates and the corresponding volatilities, first order autocorrelation, skewness, and kurtosis, when consumption growth and inflation dynamics are calibrated to the post-war data from 1947 to 2018. All asset pricing implications in population are based on simulations of 300,000 months of data. Data statistics are based on the Fama-Bliss zero-coupon database from CRSP over the sample period 1964 until 2018.

Preferences	δ	ψ	γ	ℓ	κ
	0.9990	1.5	2	1.74	0.9965
Maturity	1y	2y	3y	4y	5y
Nominal Term structure of Interest Rates - Model					
Panel A: 1964.01-2018.12					
Mean Yield (%)	5.14	5.33	5.52	5.69	5.87
Std (%)	0.83	0.79	0.74	0.71	0.68
Nominal Term structure of Interest Rates - Data					
Panel B: 1964.01-2018.12					
Mean Yield (%)	5.16	5.37	5.56	5.73	5.84
Std (%)	3.33	3.27	3.19	3.11	3.03

Table A.3: Benchmark Bond Predictability Regressions in Post-War Sample

We report model implications for predictability when consumption growth and inflation dynamics are calibrated to the post-war data from 1947 to 2018. Panel A reports the restricted Cochrane-Piazzesi regressions from the projection of holding period returns on the single CP factor; Panel B reports the Fama-Bliss regression results from the projection of holding period returns on forward-spot spreads; Panel C reports the Campbell-Shiller regressions from the projection of changes in long rate spreads on yield-spot spreads; Panel D reports the Dai-Singleton regressions from the projection of adjusted changes in long rate spreads on yield-spot spreads. Data statistics are based on the Fama-Bliss zero-coupon database from CRSP over the sample period 1964 until 2018.

Model					Data				
Panel A: Cochrane-Piazzesi: regression of holding period returns on single CP factor									
$rx_{n,t+12} = b_n \left(\gamma^\top f_t \right) + \varepsilon_{n,t+12}$									
	$n = 2$	$n = 3$	$n = 4$	$n = 5$		$n = 2$	$n = 3$	$n = 4$	$n = 5$
b_n	0.43	0.83	1.20	1.55	b_n	0.45	0.85	1.25	1.46
HH,12 lags	0.01	0.01	0.01	0.01	HH,12 lags	0.08	0.16	0.22	0.27
R^2	0.04	0.04	0.03	0.03	R^2	0.20	0.22	0.25	0.23
Panel B: Fama-Bliss: regression of holding period returns on forward-spot spread									
$rx_{n,t+12} = \alpha_n + \beta_n \left(f_{n,t} - y_{1,t}^{\$} \right) + \varepsilon_{n,t+12}$									
	$n = 2$	$n = 3$	$n = 4$	$n = 5$		$n = 2$	$n = 3$	$n = 4$	$n = 5$
β_n	0.13	0.11	0.10	0.08	β_n	0.84	1.14	1.36	1.12
HH,12 lags	0.02	0.02	0.02	0.02	HH,12 lags	0.26	0.33	0.39	0.43
R^2	0.00	0.00	0.00	0.00	R^2	0.12	0.14	0.15	0.09
Panel C: Campbell-Shiller: regression of changes in long rate spreads on yield-spot spread									
$y_{n-1,t+12}^{\$} - y_{n,t}^{\$} = \alpha_n + \beta_n \frac{1}{n-1} \left(y_{n,t}^{\$} - y_{1,t}^{\$} \right) + \varepsilon_{n,t+12}$									
	$n = 2$	$n = 3$	$n = 4$	$n = 5$		$n = 2$	$n = 3$	$n = 4$	$n = 5$
β_n	0.75	0.77	0.80	0.82	β_n	-0.67	-1.08	-1.48	-1.51
HH,12 lags	0.04	0.04	0.04	0.04	HH,12 lags	0.52	0.62	0.67	0.71
R^2	0.01	0.01	0.01	0.01	R^2	0.02	0.04	0.07	0.06
Panel D: Dai-Singleton: regression of adjusted changes in long rate spreads on yield-spot spread									
$y_{n-1,t+12}^{\$} - y_{n,t}^{\$} + \frac{1}{n-1} \hat{E}_t \left[r_{n,t+12} - y_{1,t}^{\$} \right] = \alpha_n + \beta_n \frac{1}{n-1} \left(y_{n,t}^{\$} - y_{1,t}^{\$} \right) + \varepsilon_{n,t+12}$									
	$n = 2$	$n = 3$	$n = 4$	$n = 5$		$n = 2$	$n = 3$	$n = 4$	$n = 5$
β_n	0.97	0.99	1.00	1.01	β_n	1.08	1.12	1.02	0.73
HH,12 lags	0.04	0.04	0.04	0.04	HH,12 lags	0.46	0.56	0.61	0.64
R^2	0.02	0.02	0.02	0.02	R^2	0.06	0.05	0.04	0.02

Table A.4: Benchmark Bond Predictability Regressions – Robustness

Panel A reports the restricted Cochrane-Piazzesi regressions from the projection of holding period returns on the single CP factor; Panel B reports the Fama-Bliss regression results from the projection of holding period returns on forward-spot spreads; Panel C reports the Campbell-Shiller regressions from the projection of changes in long rate spreads on yield-spot spreads; Panel D reports the Dai-Singleton regressions from the projection of adjusted changes in long rate spreads on yield-spot spreads. Data statistics are based on the Fama-Bliss zero-coupon database from CRSP over the sample period 1964 until 2018.

1964.01-1981.12					1982.01-2018.12					2009.01-2018.12				
Panel A: Cochrane-Piazzesi: regression of holding period returns on single CP factor														
$rx_{n,t+12} = b_n \left(\gamma^\top f_t \right) + \varepsilon_{n,t+12}$														
	$n = 2$	$n = 3$	$n = 4$	$n = 5$		$n = 2$	$n = 3$	$n = 4$	$n = 5$		$n = 2$	$n = 3$	$n = 4$	$n = 5$
b_n	0.40	0.84	1.24	1.52	b_n	0.48	0.86	1.23	1.43	b_n	0.29	0.72	1.25	1.74
HH,12 lags	0.08	0.15	0.20	0.25	HH,12 lags	0.09	0.18	0.27	0.33	HH,12 lags	0.03	0.04	0.06	0.15
R^2	0.15	0.24	0.28	0.26	R^2	0.23	0.19	0.20	0.17	R^2	0.79	0.86	0.87	0.83
Panel B: Fama-Bliss: regression of holding period returns on forward-spot spread														
$rx_{n,t+12} = \alpha_n + \beta_n \left(f_{n,t} - y_{1,t}^s \right) + \varepsilon_{n,t+12}$														
	$n = 2$	$n = 3$	$n = 4$	$n = 5$		$n = 2$	$n = 3$	$n = 4$	$n = 5$		$n = 2$	$n = 3$	$n = 4$	$n = 5$
β_n	0.62	1.10	1.42	1.07	β_n	0.55	0.58	0.73	0.50	β_n	1.27	1.76	2.34	2.86
HH,12 lags	0.35	0.37	0.41	0.52	HH,12 lags	0.45	0.52	0.54	0.50	HH,12 lags	0.31	0.41	0.36	0.18
NW,18 lags	0.32	0.34	0.38	0.50	NW,18 lags	0.39	0.45	0.48	0.46	NW,18 lags	0.28	0.37	0.33	0.19
R^2	0.07	0.14	0.15	0.07	R^2	0.05	0.03	0.04	0.02	R^2	0.48	0.63	0.74	0.82
Panel C: Campbell-Shiller: regression of changes in long rate spreads on yield-spot spread														
$y_{n-1,t+12}^s - y_{n,t}^s = \alpha_n + \beta_n \frac{1}{n-1} \left(y_{n,t}^s - y_{1,t}^s \right) + \varepsilon_{n,t+12}$														
	$n = 2$	$n = 3$	$n = 4$	$n = 5$		$n = 2$	$n = 3$	$n = 4$	$n = 5$		$n = 2$	$n = 3$	$n = 4$	$n = 5$
β_n	-0.24	-0.83	-1.27	-1.36	β_n	-0.09	-0.17	-0.47	-0.47	β_n	-1.54	-2.48	-3.37	-4.29
HH,12 lags	0.71	0.71	0.69	0.74	HH,12 lags	0.89	1.02	1.06	1.04	HH,12 lags	0.62	0.75	0.67	0.45
NW,18 lags	0.64	0.65	0.63	0.69	NW,18 lags	0.79	0.89	0.93	0.92	NW,18 lags	0.57	0.68	0.63	0.48
R^2	0.00	0.03	0.05	0.05	R^2	0.00	0.00	0.01	0.00	R^2	0.25	0.44	0.58	0.65
Panel D: Dai-Singleton: regression of adjusted changes in long rate spreads on yield-spot spread														
$y_{n-1,t+12}^s - y_{n,t}^s + \frac{1}{n-1} \hat{E}_t \left[r_{n,t+12} - y_{1,t}^s \right] = \alpha_n + \beta_n \frac{1}{n-1} \left(y_{n,t}^s - y_{1,t}^s \right) + \varepsilon_{n,t+12}$														
	$n = 2$	$n = 3$	$n = 4$	$n = 5$		$n = 2$	$n = 3$	$n = 4$	$n = 5$		$n = 2$	$n = 3$	$n = 4$	$n = 5$
β_n	0.91	1.04	1.02	0.88	β_n	1.20	1.21	0.94	0.64	β_n	0.82	0.89	1.03	0.95
HH,12 lags	0.78	0.77	0.72	0.79	HH,12 lags	0.73	0.90	0.94	0.96	HH,12 lags	0.33	0.25	0.05	0.16
NW,18 lags	0.70	0.68	0.65	0.72	NW,18 lags	0.65	0.79	0.82	0.84	NW,18 lags	0.30	0.24	0.12	0.26
R^2	0.05	0.05	0.04	0.03	R^2	0.07	0.05	0.03	0.01	R^2	0.20	0.23	0.23	0.13

Table A.5: Preference-based models for the Term Structure of Interest Rates

In this table, we summarize some of the key preference-based models that examine the term structure of nominal interest rates (time-separable CRRA preferences, Habit, Epstein-Zin recursive preferences, and Generalized Disappointment Aversion). We report the preference model, the key state variables for the real and nominal endowments, and the main preference parameters. The real endowment contains expected growth (x_t), time-varying volatility in expected growth (σ_t^x), time-varying volatility in realized growth (σ_t^c), jumps in consumption growth (J_t^c), surplus consumption ratio (s_t), expected inflation (z_t), volatility in expected inflation (σ_t^z), volatility in realized inflation (σ_t^π), jumps in inflation (J_t^z), and joint jumps in inflation and consumption growth ($J_t^{c,\pi}$). The reported preference parameters are the subjective discount factor δ , the coefficient of relative risk aversion γ , the coefficient of intertemporal elasticity of substitution ψ , the disappointment intensity ℓ , and the disappointment threshold κ . Wachter (2006) calibrates the subjective discount factor at a quarterly frequency with $\delta = 0.98$. Le et al. (2010) calibrate the subjective discount factor at a quarterly frequency with $\delta = 0.9904$. We relate to their calibration scheme CS in Table 1. Gabaix (2012) uses a time preference parameter ρ equal to 6.57%, which we map into a subjective discount factor at a monthly frequency of $\delta = \exp(-\rho)^{(1/12)}$ for comparability. Tsai (2016) uses a time preference parameter of 0.010 in continuous time, which we have mapped into a comparable monthly value of $\delta = \exp(-\rho \times (1/12)) = 0.9992$. Preference parameters for Creal and Wu (2020) are average estimates for the benchmark model (Table 1, global maximum).

Study	Preferences				Endowment										Benchmark Parameters				
	CRRA	Habit	EZ	GDA	x_t	σ_t^x	σ_t^c	J_t^c	s_t	z_t	σ_t^z	J_t^z	σ_t^π	$J_t^{c,\pi}$	δ	γ	ψ	ℓ	κ
Piazzesi and Schneider (2006)			✓		✓					✓					1.0050	59	1	—	—
Wachter (2006)		✓							✓	✓					0.9933	2	—	—	—
Le et al. (2010)		✓			✓				✓	✓					0.9968	2.20	—	—	—
Bansal and Shaliastovich (2013)			✓		✓	✓				✓	✓				0.9940	20.9	1.81	—	—
Gabaix (2012)	✓							✓		✓		✓			0.9945	4	—	—	—
Tsai (2016)			✓					✓		✓		✓		✓	0.9992	3	1	—	—
Creal and Wu (2020)		✓	✓		✓	✓	✓		✓	✓	✓		✓		1.002	1.70	0.8	—	—
This study				✓			✓			✓	✓				0.9985	2	1.5	1	0.95